

Dear Editor, dear Niels

We have shortened the main text from 9272 to 8373 words (c. 10%) as recommended, with the result that the paper reads better and is more concise.

Thank you very much for handling our manuscript.

Sincerely

Fritz Schlunegger, Philippos Garefalakis

1 | **Clast imbrication in coarse-grained mountain streams and stratigraphic archives**
2 | **as indicator of deposition in upper flow regime,**

geo Uni Bern 22.8.2018 10:47
Deleted: imbrications...mbricati... [1]

3
4 | Fritz Schlunegger, Philippos Garefalakis
5 | Institute of Geological Sciences
6 | University of Bern, Switzerland
7 | fritz.schlunegger@geo.unibe.ch
8 | philippos.garefalakis@geo.unibe.ch

9
10
11
12
13
14
15
16
17
18
19
20
21
22
23
24
25
26
27
28
29
30
31
32
33
34
35
36
37
38
geo Uni Bern 22.8.2018 10:47
Formatted: Font:Times, 10 pt, German (Switzerland)

11 | **Abstract**

12 | Clast imbrication is one of the most conspicuous sedimentary structures in coarse-
13 | grained clastic deposits of modern rivers but also in the stratigraphic record. In this
14 | paper, we test whether the formation of this fabric can be related to the occurrence of
15 | upper flow regime conditions in streams. To this end, we calculated the Froude number at
16 | the incipient motion of coarse-grained bedload for various values of relative bed roughness
17 | and stream gradient as these are the first order variables that can practically be extracted
18 | from preserved deposits. We found that a steeper energy gradient, or slope, and a larger
19 | bed roughness tend to favor the occurrence of supercritical flows. We also found that at
20 | the onset of grain motion, the ratio ϕ between the critical shear stress for the entrainment
21 | of a sediment particle and its inertial force critically controls whether flows tend to be
22 | super- or subcritical during entrainment. We then mapped the occurrence of clast
23 | imbrication in Swiss streams and compared these data with the hydrologic calculations.
24 | Results indicate that imbrication may record supercritical flows provided that (i) ϕ -values
25 | are larger than c. 0.05, which is appropriate for streams in the Swiss Alps; (ii) average
26 | stream gradients exceed c. $0.5 \pm 0.1^\circ$; and (iii) relative bed roughness values, i.e. the ratio
27 | between water depth d and bed sediment D_{b4} , are larger than -0.06 ± 0.01 . We cannot rule
28 | out that imbrication may be formed during subcritical flows with ϕ -values as low as 0.03,
29 | as demonstrated in a large number of flume experiments. However, our results from Alpine
30 | streams suggest that clast imbrication likely reflects upper flow regime conditions, where
31 | clasts form well sorted and densely packed clusters. We consider that these differences
32 | may be rooted in a misfit between the observational and experimental scales.

geo Uni Bern 22.8.2018 10:47
Deleted: imbrications are...mbrica... [2]

34 | **1 Introduction**

35 | Conglomerates, representing the coarse-grained spectrum of clastic sediments, bear
36 | key information about the provenance of the material (Matter, 1964), the sedimentary
37 | environments (Rust, 1978; Middleton and Trujillo, 1984), and the hydro-climatic
38 | conditions upon transport and deposition (Duller et al., 2012; D'Arcy et al., 2017).

geo Uni Bern 22.8.2018 10:47
Deleted: environment in which these sediments were deposited...edimen... [3]

74 Conglomerates display the entire range of sedimentary structures including a massive-
75 bedded fabric, cross-beds and horizontal stratifications. However, the most striking
76 feature is clast imbrication (Figure 1A), which refers to a depositional fabric where
77 sediment particles of similar sizes overlap each other, similar to a run of toppled
78 dominoes (e.g., Pettijohn, 1957; Yagishita, 1997; Rust, 1984; Potsma and Roep, 1985;
79 Todd, 1996). Imbrication may lead to armor development and the interlocking of clasts.
80 As a consequence the search for possible controls on this fabric has received major
81 attention in the literature (e.g., Bray and Church, 1980; Carling, 1981; Aberle and
82 Nikora, 2006).

83 In the past decades, clast imbrication in streams has been considered to record high
84 stage flows (Rust, 1978; Miall, 1978; Sinclair and Jaffey, 2001). This could occur in the
85 upper flow regime, where the flow velocity of a stream v exceeds the wave's celerity c
86 (Allen, 1997), i.e. the speed of a wave on the water surface. The ratio v/c of these
87 velocities has been referred to as the Froude number F where, in theory, $F > 1$ denotes an
88 upper flow regime or a supercritical flow, while $F < 1$ is characteristic for a lower flow regime
89 or a subcritical flow (Engelund and Hansen, 1967). A hydraulic jump, which is
90 characterized by a distinct increase in flow surface elevation and a decrease in flow
91 velocity, marks the downstream transition from a super- to a subcritical flow (Figure 1A).
92 This hydrological condition is particularly mirrored by the surface texture in relation to
93 water depth. Surface waves of subcritical flows have wavelenghts that are smaller than
94 water depths (Figure 1B). The surface waves tend to migrate and fade out in the upstream
95 direction with respect to the flow. Contrariwise, the wavelength of a standing wave, which
96 is a feature of a supercritical flow ($F \approx 1$), is larger than water depth, and the surface wave is
97 stationary (supplement). Hydraulic jumps are manifested by a sudden decrease of the flow
98 velocity and by an overturning of the flow surface (Figure 1).

99 Significant sediment accumulation may occur underneath the hydraulic jump upon
100 deceleration of the flow's velocity (Slootman et al., 2018). Contrariwise, a downstream
101 change from a lower to an upper flow regime has no distinct surface expression, neither in
102 terms of flow depth nor flow surface texture. While these mechanisms have been well
103 explored and reported both from modern environments (e.g., Figure 1) and fine grained
104 stratigraphic records (Alexander et al., 2001; Schlunegger et al., 2017; Slootman et al.,
105 2018) and illustrated on photos from the field (Spreafacio et al., 2001), less evidence for a
106 supercritical flow has been documented from conglomerates. This even led Grant (1997)
107 to note that supercritical flows in fluvial channels are rare, and that the use of the Froude
108 number lacks justification from sedimentary records. In addition, Jarrett (1984) and Trieste
109 (1992, 1994) considered that reports of inferred upper flow regimes might be biased by
110 underestimations of the bed roughness in mountain streams. Nevertheless, the surface
111 texture of the flow illustrated in Figure 1A is characteristic for many streams (Spreafico et
112 al., 2001), where hydraulic jumps are observed on the stoss side of large imbricated clasts.

geo Uni Bern 22.8.2018 10:47

Deleted: possible...sedimentary ... [4]

geo Uni Bern 22.8.2018 10:47

Deleted: the occurrence of ...last ... [5]

geo Uni Bern 22.8.2018 10:47

Deleted: occurs gradually and ...a ... [6]

162 Furthermore, because the shift of large clasts such as cobbles and boulders does involve
 163 large shear stresses and thus high discharge flows (Rust, 1978; Miall, 1978; Sinclair and
 164 Jaffey, 2001), the deposition of these particles, and particularly the formation of an
 165 imbricated fabric, is likely to occur during supercritical flows. Here, we explore the validity
 166 of this hypothesis for modern coarse-grained streams and stratigraphic records, and we
 167 calculate the related hydrological conditions. Similar to Grant (1997), we determine the
 168 Froude number at the incipient motion of coarse-grained bedload for various bed
 169 roughness and stream gradient values. We compare these results with data from modern
 170 streams in the Swiss Alps, stratigraphic records and published laboratory experiments.

172 2 Methods

173 2.1 Expressions relating flow regime to channel gradient and bed roughness

174 Channel depth and grain size are the simplest variables that can be extracted from
 175 stratigraphic records (Duller et al., 2012). These variables can additionally be used, to
 176 calculate palaeo-slope and roughness values of streams for the geologic past (Paola and
 177 Mohring, 1996; Duller et al., 2012; Schlunegger and Norton, 2015; Garefalakis and
 178 Schlunegger, 2018), and they form the basis to related channel depth and grain size to
 179 flow strength and sediment transport. We therefore decided to focus on the simplest
 180 expressions that can also be applied to geological records. We are aware that this requires
 181 large generalizations and simplifications, which will not consider the entire range of
 182 hydrological complexities.

184 2.2 Boundary conditions

185 In the following, we consider the hydrological situation at the incipient motion of coarse-
 186 grained bedload. For these conditions, the dimensionless Shields parameter ϕ can be
 187 computed, which is the ratio between the shear stress exerted by the fluid on the bed
 188 τ_{cDi} at the onset of motion of a sediment particle with a distinct grain size D_i , and the
 189 inertial force of this grain (Shields, 1936; Paola et al., 1992; Paola and Mohring, 1996;
 190 Tucker and Slingerland, 1997):

$$191 \phi = \frac{\tau_{cDi}}{(\rho_s - \rho)gD_i} \quad (1a).$$

192 Here, the constants ρ_s (2700 kg/m³) and ρ denote the sediment and water densities,
 193 and g is the gravitational acceleration. The relationship expressed in equation (1a)
 194 predicts that a sediment particle with diameter D_i will be transported if the ratio
 195 between the fluid's shear stress τ_{cDi} and the particle's inertial force equals ϕ .
 196 Assignments of values to ϕ vary considerably and range between c. 0.03 and 0.06,
 197 depending on the site-specific arrangement, the sorting, and the interlocking of the clasts
 198 (Buffington and Montgomery, 1997; Church, 1998). This also includes the hiding and

- geo Uni Bern 22.8.2018 10:47
Deleted: In addition
- geo Uni Bern 22.8.2018 10:47
Deleted: entrainment
- geo Uni Bern 22.8.2018 10:47
Deleted:
- geo Uni Bern 22.8.2018 10:47
Deleted: it is possible that the transport and
- geo Uni Bern 22.8.2018 10:47
Deleted: may
- geo Uni Bern 22.8.2018 10:47
Deleted: conditions of
- geo Uni Bern 22.8.2018 10:47
Deleted: then
- geo Uni Bern 22.8.2018 10:47
Deleted: the
- geo Uni Bern 22.8.2018 10:47
Deleted: results of
- geo Uni Bern 22.8.2018 10:47
Deleted: and most straightforward
- geo Uni Bern 22.8.2018 10:47
Deleted: It has been shown that quantitative information about these
- geo Uni Bern 22.8.2018 10:47
Deleted: as basis
- geo Uni Bern 22.8.2018 10:47
Deleted:). We therefore decided to focus on the simplest expressions relating
- geo Uni Bern 22.8.2018 10:47
Deleted: , such as
- geo Uni Bern 22.8.2018 10:47
Deleted: the resulting formulas
- geo Uni Bern 22.8.2018 10:47
Deleted: will be associated with
- geo Uni Bern 22.8.2018 10:47
Deleted: that are usually associated with the transport of coarse-grained bedload in streams
- geo Uni Bern 22.8.2018 10:47
Deleted: particle's
- geo Uni Bern 22.8.2018 10:47
Deleted: at the incipient motion
- geo Uni Bern 22.8.2018 10:47
Formatted: Expanded by 0.2 pt
- geo Uni Bern 22.8.2018 10:47
Deleted: $\phi = \frac{\tau_{cDi}}{(\rho_s - \rho)gD_i}$
- geo Uni Bern 22.8.2018 10:47
Deleted: Here, τ_{cDi} denotes the critical shear stress, or alternatively the Shields stress, which is required to shift a ... [7]
- geo Uni Bern 22.8.2018 10:47
Deleted: the value of
- geo Uni Bern 22.8.2018 10:47
Deleted: largely

234 protrusion of small and large clasts, respectively, which exert a strong influence on the
235 thresholds for clast entrainment (e.g., Egiazaroff, 1965; Parker et al., 1982; Andrews,
236 1984; Kirchner et al., 1990). Likewise, a smooth channel bed surface, such as a well-
237 armored channel floor with well-sorted clasts, is likely to offer a greater resistance for the
238 entrainment of a sediment particle than a gravel bar with poorly sorted material (Egiazaroff,
239 1965; Buffington and Montgomery, 1997).

240 The relationships denoted in equation (1a) differ for channel forming floods, where channel
241 forming Shield stresses $\tau_{channel}$ are up to 1.2 times (Parker, 1978) above the threshold τ_{cDi}
242 for the onset of grain motion. Pfeiffer et al. (2017) additionally showed that some rivers
243 have a $\tau_{channel}/\tau_{cDi}$ ratio that is even higher. The consideration of channel forming floods
244 thus requires larger thresholds;

$$245 \quad \phi' \geq \frac{\tau_{channel}}{(\rho_s - \rho)gD_i} \approx 1.2 \frac{\tau_{cDi}}{(\rho_s - \rho)gD_i} = 1.2\phi \quad (1b).$$

246 Accordingly, the critical shear stress τ_{cDi} for the entrainment of a sediment particle with a
247 distinct grain size D_i can be computed through:

$$248 \quad \tau_{cDi} = \phi(\rho_s - \rho)gD_i \quad (2).$$

249 Among the various grain sizes, the D_{84} has been considered as more representative for,
250 the gravel bar structure than the D_{50} (Howard, 1980; Hey and Thorne, 1986; Grant et
251 al., 1990). In addition, the D_{84} has also been used for the quantification of the relative
252 bed roughness, which is the ratio between grain size and water depth (e.g., Wiberg and
253 Smith, 1991). If this inference is valid, then a major alteration of channel-bar
254 arrangements requires a flow that is strong enough to entrain the D_{84} grain size.

255 A Shields variable of $\phi=0.047$, which is based on flume experiments (Meyer-Peter and
256 Müller, 1948) and observations in the field (Andrews, 1984), has conventionally been
257 employed in a large number of studies (e.g., Paola and Mohring, 1996) particularly if
258 the D_{50} is considered. Note that a re-analysis (Wong and Parker, 2006) of the Meyer-
259 Peter and Müller (1948) data returned a value of $\phi=0.0495 \approx 0.05$, which we employed
260 in this paper. However, experiments also showed that material transport can occur at a
261 lower threshold with a ϕ -value are as low as 0.03 (Ferguson, 2012; Powell et al., 2016).
262 This might particularly be an appropriate threshold for the entrainment of the D_{84} ,
263 because of possible protrusion effects (e.g., Kirchner et al., 1990). Alternatively, Mueller
264 et al. (2005) and Lamb et al. (2008) proposed that ϕ depends on channel gradient, where
265 ϕ (for the D_{50} grain size) might exceed 0.1 for channels steeper than 1.1° . It appears that
266 the threshold for the onset of grain motion varies depending on site and experiment
267 specific conditions. We therefore employed the entire range of ϕ -values from 0.03 to
268 1.1 to comply with these complexities, which also includes channel forming floods
269 (Parker, 1978).

270

geo Uni Bern 22.8.2018 10:47

Deleted: may ...xert a strong influ... [8]

geo Uni Bern 22.8.2018 10:47

Deleted: the case of ...hannel form... [9]

geo Uni Bern 22.8.2018 10:47

Deleted: Equation (1a) can then be transformed to an expression, which quantifies...ccordingly, the critical... [10]

geo Uni Bern 22.8.2018 10:47

Deleted: grain size ...as been... [11]

geo Uni Bern 22.8.2018 10:47

Deleted: Based on the results of... [12]

322 2.3 Hydrology, bed shear stress and onset of grain motion,

323 Bed shear stress is calculated using an approximation for a steady, uniform flow down an
324 inclined plane, where channel width is more than 20 times larger than water depth (e.g.
325 Tucker & Slingerland, 1997):

$$326 \tau = g\rho Sd \quad (3).$$

327 Here, S denotes channel gradient, and d is water depth.

328 Alternatively, bed shear stress can also be computed as a function of the kinetic energy
329 represented by the flow velocity v (Ferguson, 2007):

$$330 \tau = \frac{f}{8} \rho v^2 \quad (4).$$

331 The variable f , referred to as the Darcy-Weisbach friction factor (e.g., Papaevangelou et al.,
332 2010), is a measure for the friction effect within the roughness layer at the flow bottom
333 (Krogstad and Antonia, 1999). It also considers skin friction within the flow column
334 (Ferguson, 2007). Ferguson (2007) reduced these complexities to a single expression,
335 where f depends on water depth d relative to the grain size D_{84} and thus on the relative
336 bed roughness:

$$337 \frac{f}{8} = \left(\frac{D_{84}}{d}\right)^2 + \left(\frac{D_{84}}{d}\right)^{1/3} \quad (5).$$

338 Here, a_1 and a_2 are constants that vary between 7–8 and 1–4, respectively (Ferguson,
339 2007), which have been calibrated to $a_1 = 7.5$ and $a_2 = 2.36$ (Ferguson, 2007). We
340 additionally considered possible consequences of energy loss through assignments of
341 different values to the Shields (1936) variable (see explanation of equation 1a above). We
342 are aware that we could also employ the Manning's number n for the characterization of
343 the channel's fabric (Whipple, 2004) and the relative bed roughness (Jarrett, 1984).
344 Related expressions (Jarrett, 1984) predict that n hinges on channel gradient and
345 water depth only and not on bed structure. We thus prefer to use Ferguson's (2007)
346 approach (eq. 5), which explicitly considers the relative bed roughness, consistent with
347 the most recent work by Wickert and Schildgen (2018, see their equation 13).

348 As outlined in the introduction, the Froude number F depends on the ratio of flow velocity v
349 and surface wave celerity c . For shallow waters, which is commonly the case for rivers and
350 streams, this relationship can be computed if water depth d is known:

$$351 F = \frac{v}{c} = \frac{v}{\sqrt{gd}} \quad (6).$$

352 The combination of equations 3, 4, and 6 then yields a simple expression where:

$$353 F = \sqrt{8 \frac{S}{f}} \quad (7).$$

geo Uni Bern 22.8.2018 10:47

Deleted: stresses...tress and ... [13]

geo Uni Bern 22.8.2018 10:47

Deleted: the...n approximation fo ... [14]

geo Uni Bern 22.8.2018 10:47

Deleted: the ...hannel gradient, a ... [15]

geo Uni Bern 22.8.2018 10:47

Deleted: stresses...tress can also ... [16]

geo Uni Bern 22.8.2018 10:47

Deleted: In this relationship, v is the flow velocity. ...he variable f , referred to ... [17]

geo Uni Bern 22.8.2018 10:47

Deleted:). A calibration of equation 5 by Ferguson (2007), where the D_{84} was employed as the threshold grain size, returned values of 7.5 and 2.36 for a_1 and a_2 , respectively, which we adapt in this paper...., which have been calibrat ... [18]

geo Uni Bern 22.8.2018 10:47

Deleted: can be approximated ... [19]

geo Uni Bern 22.8.2018 10:47

Deleted: Combining equation...h ... [20]

422 This expression states that the Froude number F_v depends on two partly non-related
 423 variables. In particular, for a given bed friction f , an upper flow regime tends to
 424 establish for steep channels. Contrariwise, a lower regime is maintained where poorly
 425 sorted material exerts a large resistance on the flow, thereby reducing the flow velocity
 426 and hence the Froude number. Accordingly, the dependency of F on channel gradient S
 427 can be computed through the combination of equations 2, 3, 5 and 7:

$$428 \quad F = \sqrt{\frac{S}{\left(\frac{\rho S}{\phi(\rho_s - \rho)}\right)^2 * a_2^{-2} + \left(\frac{\rho S}{\phi(\rho_s - \rho)}\right)^{1/3} * a_1^{-2}}} \quad (8).$$

429 Alternatively, an expression where the Froude number depends on the bed roughness
 430 D_{84}/d only can be achieved through the combination of equations 2, 3 and 7:

$$431 \quad F = \sqrt{8 * \frac{\phi(\rho_s - \rho)}{\rho * f} * \frac{D_{84}}{d}} \quad (9).$$

432 We thus used equations 8 and 9 to calculate the Froude numbers at the onset of motion
 433 of the D_{84} grain size. We then compared these results with data from modern streams and
 434 stratigraphic records.

436 2.4 Collection of data from modern streams and stratigraphic records

437 We used observations about clast arrangements in gravelly streams in Switzerland. We
 438 paid special attention to the occurrence of clast imbrication, as we hypothesize that this
 439 fabric may document the occurrence of an upper flow regime (Figure 1) upon
 440 sedimentation and gravel bar migration. We explored multiple gravel bars for the
 441 occurrence or absence of clast imbrication over a reach of several hundreds of meters,
 442 where Litty and Schlunegger (2017) reported grain size data (Table 1). We then
 443 determined a mean energy gradient over a c. 500 m-long reach, which we calculated from
 444 topographic maps at scales 1:10'000.

445 The selected streams are all situated around the Central Alps (Figure 2), have different
 446 source rock lithologies (Spicher, 1980) and grain size distributions. At sites where grain
 447 size data has been collected, the ratio between the clasts' medium b - and longest a -axes
 448 is constant and ranges between 0.67 and 0.72 irrespective of the grain size distribution in
 449 these streams (Litty and Schlunegger, 2017). For these sites, we calculated the bed
 450 roughness D_{84}/d at the incipient motion of the D_{84} . Here, related water depths d were
 451 determined through the combination of equations (2) and (3), and using the channel
 452 gradient S at these sites.

453 The Swiss Federal Office for the Environment (FOEN) estimated the Froude numbers for
 454 various flood magnitudes of streams on the northern side of the Swiss Alps (Spreafico et
 455 al., 2001; see Figure 2 for location of sites). These estimates are based on flow velocities,
 456 flow depths and cross-sectional geometries of channels. The authors of this study also

- geo Uni Bern 22.8.2018 10:47
Deleted: flow regime, expressed here by the
- geo Uni Bern 22.8.2018 10:47
Deleted: ,
- geo Uni Bern 22.8.2018 10:47
Deleted: which depends on the bed roughness (Ferguson, 2007),
- geo Uni Bern 22.8.2018 10:47
Deleted: conditions tend
- geo Uni Bern 22.8.2018 10:47
Deleted: flows may occur in a steep environment
- geo Uni Bern 22.8.2018 10:47
Deleted: where the entrainment of sediment particles can be expressed through the Shields (1936) variable ϕ ,
- geo Uni Bern 22.8.2018 10:47
Deleted: the
- geo Uni Bern 22.8.2018 10:47
Deleted: , also during channel forming floods
- geo Uni Bern 22.8.2018 10:47
Deleted: incipient
- geo Uni Bern 22.8.2018 10:47
Deleted: sizes
- geo Uni Bern 22.8.2018 10:47
Deleted: imbrications
- geo Uni Bern 22.8.2018 10:47
Deleted: regimes
- geo Uni Bern 22.8.2018 10:47
Deleted: We selected those sites for which Litty and Schlunegger (2017) reported grain size data (Table 1). At these locations, we
- geo Uni Bern 22.8.2018 10:47
Deleted: imbrications
- geo Uni Bern 22.8.2018 10:47
Deleted: .
- geo Uni Bern 22.8.2018 10:47
Deleted: various upstream drainage basins and
- geo Uni Bern 22.8.2018 10:47
Deleted: are
- geo Uni Bern 22.8.2018 10:47
Deleted: range
- geo Uni Bern 22.8.2018 10:47
Deleted: selected
- geo Uni Bern 22.8.2018 10:47
Deleted: situated

487 determined the corresponding channel gradient over a reach of several hundred meters.
488 We will thus use the Spreafico et al. (2001) dataset to constrain the range of possible ϕ
489 values for streams in Switzerland.

490 We finally identified relationships between channel gradient, bed roughness, and clast
491 imbrication from stratigraphic records. We focused on the Late Oligocene suite of alluvial
492 megafan conglomerates (Rigi and Thun sections, Figure 2) deposited at the proximal
493 border of the Swiss Molasse basin. For these conglomerates, Garefalakis and
494 Schlunegger (2018) and Schlunegger and Norton (2015) collected data about the depth
495 and gradient of palaeo-channels, and information about the grain size distribution along c.
496 3000 to 3600 m-thick sections (Table 1). We returned to these sections and examined c.
497 50 sites for the occurrence of clast imbrication within the conglomerate suites.

499 3 Results

500 3.1 Calculation of flow regime as a function of bed roughness and channel gradient

501 We calculated the Froude numbers F for different channel gradient S and bed roughness
502 D_{84}/d values, and thresholds ϕ for the incipient motion of material. We compared these
503 results with observations from modern streams and stratigraphic records. We avoided
504 calculation of the Froude numbers for slopes steeper than 1.4° because channels tend to
505 adapt a step-pool geometry in their thalwegs (Whipple, 2014), for which our calculations no
506 longer apply. We set the thresholds for a critical flow to a Froude number $F=0.9$, which is
507 consistent with estimations for the formation of upper flow regime bedforms by Koster
508 (1978). Calculations were initially carried out using $\phi=0.0495\approx 0.05$, as this value has
509 commonly been used in a large number of studies (see above). The results reveal that F
510 increases with steeper channels (Figure 3A) and reaches the field of a critical flow for
511 $\sim 0.5^\circ$ slopes. The values reach a maximum of $F\approx 1$ where channel gradients are between
512 $\sim 0.8^\circ - 1^\circ$. Froude numbers F then slightly decrease for channels steeper than 1° and finally
513 reach a value of 0.9 for gradients $> 1.2^\circ$. In the case of a greater threshold for the onset of
514 grain motion, expressed through $\phi = 0.06$, flows adapt supercritical conditions for channels
515 steeper than $\sim 0.4^\circ$. For a lower threshold, expressed here through $\phi = 0.03$, streams remain
516 in the lower flow regime.

517 The Froude number pattern is quite similar for increasing bed roughness (Figure 3B). For
518 $\phi = 0.0495\approx 0.05$, the Froude numbers increase with higher relative bed roughness.
519 Supercritical conditions are reached for a bed roughness of c. 0.1, after which the Froude
520 numbers decrease with larger roughness. For $\phi = 0.06$, an upper flow regime might prevail
521 for bed surface roughness values between 0.06 and 0.5. Smaller and larger roughness
522 values will keep the flow in the lower regime. Contrariwise, the flow will not shift to the
523 upper regime for ϕ -values as low as 0.03. Note that the consideration of the full range of
524 roughness-layer and skin friction effects, expressed through the coefficients a_1 and a_2 in

geo Uni Bern 22.8.2018 10:47

Deleted: Because we will calculate the dependency of the Froude number on the channel gradient and the thresholds for the entrainment of sediment, expressed through different ϕ -values, we will

geo Uni Bern 22.8.2018 10:47

Deleted: possible ...relationships ... [21]

geo Uni Bern 22.8.2018 10:47

Deleted: regimes

geo Uni Bern 22.8.2018 10:47

Deleted: values of ...hannel grad ... [22]

geo Uni Bern 22.8.2018 10:47

Deleted: threshold conditions expressed through a Shields (1936) variable ... [23]

577 equation (8), shifts the pattern of Froude numbers to lower and higher values. But this will
578 not alter the general finding that at the onset of grain motion an upper flow regime is
579 expected for a channel gradient S , steeper than $0.5^\circ \pm 0.1^\circ$, and for a bed roughness D_{84}/d
580 greater than ~ 0.06 .

581 We also calculated the Froude numbers for $\phi = 0.1$, because observations have shown that
582 thresholds for the entrainment of sediment particles increase with steeper channels
583 (Mueller et al., 2005; Ferguson, 2012). This might be an exaggeration (Lamb et al., 2008),
584 but will give an upper bound for the dependence of the Froude number F on the Shields
585 variable ϕ . We additionally considered the case where ϕ depends on S through
586 $\phi = 2.81 * S + 0.021$ (Mueller et al., 2005). These relationships have been established based
587 on bed load rating curves for mountain streams in North America and England. We found
588 that the flows shift to critical conditions for channels steeper than between 0.5° and 0.6°
589 (slope dependent ϕ) and for a bed roughness > 0.04 ($\phi = 0.1$).

590 In summary, the calculations predict that water flow may shift to an upper flow regime for:
591 (i) ϕ -values greater than 0.05; (ii) slopes steeper than $\sim 0.5^\circ \pm 0.1^\circ$; and (iii) relative bed
592 roughness values greater than $\sim 0.06 \pm 0.01$.

593

594 3.2 Estimates of ϕ -values from modern streams in the Central Alps

595 Spreafico et al. (2001) estimated the Froude numbers for various streams situated on the
596 northern side of the Swiss Alps. The F -values range between 0.2 and 1.1 and generally
597 increase with channel gradients (vertical bars on Figure 3A). The flow's surfaces
598 particularly of the Birse and Thur streams (labeled as b and t on Figure 3A) are
599 characterized by multiple hydraulic jumps (Spreafico et al., 2001, p. 71 and p. 77).
600 Therefore, the inferred small Froude numbers (between 0.6 and 0.9) of these streams
601 have to be treated with caution.

602 The Froude number estimates by Spreafico et al. (2001) disclose a large scatter in the
603 relationship to channel gradient (Figure 3A, vertical bars). This can partially be explained
604 by site-specific differences in bed roughness due to anthropogenic corrections and
605 constructions (Spreafico et al., 2001). Nevertheless, the comparison between these data
606 and the results of our calculations reveal that the entire range of ϕ -values between 0.03
607 and 0.1 has to be taken into account for the hydrological conditions in the streams
608 surrounding the Swiss Alps (Figure 3A). This also implies that the selection of a threshold,
609 expressed by the ϕ -value, warrants a careful justification, which we present in the
610 discussion.

611

612 3.3 Occurrence or absence of clast imbrication in modern streams

613 Here, we present evidence for imbrication and non-imbrication from modern rivers,
614 situated both in the core of the Swiss Alps and the foreland, which we relate to channel

geo Uni Bern 22.8.2018 10:47

Deleted: values

geo Uni Bern 22.8.2018 10:47

Deleted: conditions at the incipient motion of gravels might be

geo Uni Bern 22.8.2018 10:47

Deleted: gradients

geo Uni Bern 22.8.2018 10:47

Deleted: that are

geo Uni Bern 22.8.2018 10:47

Deleted: a Shields variable of

geo Uni Bern 22.8.2018 10:47

Deleted: may

geo Uni Bern 22.8.2018 10:47

Deleted: .

geo Uni Bern 22.8.2018 10:47

Deleted: the Shields (1936) variable

geo Uni Bern 22.8.2018 10:47

Deleted: the channel gradient

geo Uni Bern 22.8.2018 10:47

Deleted: using

geo Uni Bern 22.8.2018 10:47

Deleted: , which are based on field surveys in mountainous

geo Uni Bern 22.8.2018 10:47

Deleted: conditions

geo Uni Bern 22.8.2018 10:47

Deleted: larger

geo Uni Bern 22.8.2018 10:47

Deleted: Related

geo Uni Bern 22.8.2018 10:47

Deleted: together

geo Uni Bern 22.8.2018 10:47

Deleted: The surface expressions of the flows

geo Uni Bern 22.8.2018 10:47

Deleted: the

geo Uni Bern 22.8.2018 10:47

Deleted: , which are related

geo Uni Bern 22.8.2018 10:47

Deleted: Data about the occurrence

geo Uni Bern 22.8.2018 10:47

Deleted: imbrications from

geo Uni Bern 22.8.2018 10:47

Deleted: imbrications

geo Uni Bern 22.8.2018 10:47

Deleted: imbrications

geo Uni Bern 22.8.2018 10:47

Deleted: , and

geo Uni Bern 22.8.2018 10:47

Deleted: these observations

642 | slope (Figure 4A) and bed roughness (Figure 4B). The bedrock-geology of the
643 | headwaters includes the entire range of lithologies from sedimentary units to schists,
644 | gneisses and granites. In addition, the streams cover the full range of water sources,
645 | including glaciers and surface runoff. Except for the Maggia River between the sites
646 | Bignasco and Losone (Figure 2), all streams are channelized by artificial riverbanks. These
647 | are either made up of concrete walls or oversized boulders. Information about the
648 | hydrographs, grain size and the results of the shear stress calculations consider the time
649 | after these constructions have been made.

650 | *Channel morphologies*

652 | The thalweg of the streams meanders between the artificial walls within a 20 to 50 m-wide
653 | belt. Flat-topped longitudinal bars that are several tens of meters long and that emerge up
654 | to 1.5 m above the thalweg are situated adjacent to the artificial riverbanks on the slip-off
655 | slope of these meanders. They evolve into subaquatic transverse bars, or riffles, farther
656 | downstream where the thalweg shifts to the opposite channel margin. Channels are
657 | deepest and flattest along the outer cutbank side of the meanders and in pools
658 | downstream of riffles, respectively. The thalweg then steepens where it crosses the
659 | transverse bars and riffles. This is also the location where some streams show evidence
660 | for standing waves with wavelengths >5 m (e.g., at Reuss, Figure 5). Standing waves have
661 | also been encountered in the Waldemme River at Littau (Figure 6B; see supplement)
662 | when water runoff at that particular site was c. 100 m³/s and when rumbling sounds
663 | indicated that clasts were rolling or sliding. The streams thus display a complex pattern
664 | where channel depths, flow velocities and hydrological regimes alternate over short
665 | distances of tens to hundreds of meters. These arrangements of channel-bar pairs and
666 | particularly their positions within the channel belt has been stable over the past years
667 | because the gravel bars are situated in the same locations as the ones reported by Litty
668 | and Schlunegger (2016).

669 | *Streams with evidence for clast imbrication*

671 | Inspections of gravel bars have shown clear evidence for imbrication in the Glenner, the
672 | Landquart, the Verzasca, and the Waldemme rivers (Table 1). In these streams, channel
673 | gradients range between 0.6° (Waldemme) and 1.2° (Glenner) (Figure 4A). The sizes of
674 | the D_{84} range between 3 cm (Waldemme) and 12 cm (Glenner). The gravel lithology
675 | includes the entire variety from sedimentary (Waldemme) to crystalline constituents
676 | (Glenner, Landquart, Verzasca). The inferred bed roughness at the onset of motion of the
677 | D_{84} includes the range between c. 0.125 (Waldemme) and 0.31 (Glenner) (Figure 4B). In
678 | these streams, bars with imbricated clasts alternate with pools over a reach of several
679 | hundreds of meters.

geo Uni Bern 22.8.2018 10:47

Deleted: Data on grain size, stream runoff and channel morphology are available for several rivers in the northern, the central and the southern part of the Swiss mountain belt. These streams are situated both in the core of the Alps and the foreland.

geo Uni Bern 22.8.2018 10:47

Deleted: their

geo Uni Bern 22.8.2018 10:47

Deleted: the same sense

geo Uni Bern 22.8.2018 10:47

Deleted: in their headwaters

geo Uni Bern 22.8.2018 10:47

Deleted: , and the rivers generally flow in a bed that is laterally confined

geo Uni Bern 22.8.2018 10:47

Deleted: In this context, information

geo Uni Bern 22.8.2018 10:47

Deleted: suggested

geo Uni Bern 22.8.2018 10:47

Deleted: possibly also

geo Uni Bern 22.8.2018 10:47

Deleted: as the locations of

geo Uni Bern 22.8.2018 10:47

Deleted: still

geo Uni Bern 22.8.2018 10:47

Deleted: imbrications

geo Uni Bern 22.8.2018 10:47

Deleted: incipient

699 At Maggia, Reuss and Waldemme Littau, the largest clasts are arranged as triplets or
700 quadruplets of imbricated constituents within generally flat lying to randomly-oriented finer
701 grained sediment particles. The density of these arrangements ranges between 5 groups
702 per 10 m² (Maggia Bignasco, Maggia Losone) to c. 10 groups per 10 m² (Maggia Visletto,
703 Reuss, Waldemme Littau e.g. Figure 6D). The channel gradients at these sites span the
704 range between c. 0.3 and 0.6°, and the D_{84} clasts are between 3 and 9 cm large (Reuss
705 and Maggia Visletto). Accordingly, the relative bed roughness at the incipient motion of the
706 D_{84} ranges between 0.07 and 0.16.

707 At all sites mentioned above, clasts on subaquatic and subaerial gravel bars are generally
708 arranged as well-sorted and densely packed clusters, possibly representing incipient
709 bedforms (e.g., Figure 6D). In most cases, grains imbricate behind an outsized clast, which
710 usually delineates the front of imbricated grains. In addition, the lowermost 10-20% part of
711 most of the large clasts is embedded, and thus buried, in a fine-grained matrix, which was
712 most likely deposited during the waning stage of a flood. Isolated, non-buried clasts that
713 are flat lying on their *a-b*-planes are less frequent than embedded clasts or constituents
714 arranged in clusters. The inclination dip of the *a-b*-planes ranges between c. 20-40°
715 (Figure 6D). Finally, streams with clast imbrications display surface expressions, which
716 point to an upper flow regime during low (e.g., Reuss, Figure 5B) and high-water stages
717 (e.g., Waldemme, Figure 6B, see supplement).

718

719 *Streams with little or no evidence for clast imbrication*

720 Gravel bars within the Emme stream are made up of generally flat lying gravels and
721 cobbles. A small tilt ($<10^\circ$) of *a-b*-planes occurs where individual clasts slightly overlap
722 each other, similar to a shingling arrangement of particles. This is particularly the case in
723 pools and on the upstream stoss-side of longitudinal and transverse bars where channel
724 gradients are flat. Also in the Emme River, clast imbrication occurs in places only where
725 gravel bars have steep downstream slip faces, which are mainly observed at the end of
726 transverse bars. At sites where imbrication is absent, most of the clasts are lying flat on
727 their *a-b*-planes, and embedding by finer-grained material is less frequently observed than
728 in streams with clast imbrication. The channel gradient is less than 0.5°, and the size of the
729 D_{84} measures 2 cm. The bed roughness of this stream, calculated for the incipient of
730 motion of the 84th grain size percentile, ranges between 0.07 and 0.10. Finally, the flow
731 has a smooth surface during low- and high-water stages (Spreafico et al., 2001, p. 53),
732 which points to a lower flow regime.

733 The Sense River differs from the Emme stream in the sense that bedrock reaches
734 alternate with alluvial segments over 100-200 meters and more. Alluvial segments are flat
735 (c. 0.3°) and host lateral and transverse gravel bars where the D_{84} measures 6 cm. On top
736 of these bars, gravels generally rest flat on their *a-b*-planes (Figure 6C). Imbrication is
737 observed where some of these gravels overlap each other, resulting in a dip angle of 10-

geo Uni Bern 22.8.2018 10:47

Deleted: arrangements of sediment particles.

geo Uni Bern 22.8.2018 10:47

Deleted: do occur but

geo Uni Bern 22.8.2018 10:47

Deleted: of <

geo Uni Bern 22.8.2018 10:47

Deleted: °

geo Uni Bern 22.8.2018 10:47

Deleted: imbrications occur

geo Uni Bern 22.8.2018 10:47

Deleted: imbrications

geo Uni Bern 22.8.2018 10:47

Deleted: displays

geo Uni Bern 22.8.2018 10:47

Deleted: expression

geo Uni Bern 22.8.2018 10:47

Deleted: is

geo Uni Bern 22.8.2018 10:47

Deleted: characteristic evidence for

geo Uni Bern 22.8.2018 10:47

Deleted: conditions

geo Uni Bern 22.8.2018 10:47

Deleted: channel morphology of the

geo Uni Bern 22.8.2018 10:47

Deleted: that of

geo Uni Bern 22.8.2018 10:47

Deleted: a wavelength of

geo Uni Bern 22.8.2018 10:47

Deleted: are

geo Uni Bern 22.8.2018 10:47

Deleted: lying

geo Uni Bern 22.8.2018 10:47

Deleted: Imbrications are

geo Uni Bern 22.8.2018 10:47

Deleted: are overlapping

757 20°. Contrariwise, bedrock reaches (site S' on Figure 4A) that form distinct steps in the
758 thalweg, are up to 0.5° steep and partly covered by subaquatic longitudinal bars (Figure
759 1B) where imbricated clasts alternate with flat-lying grains at the meter scale. The channel
760 bed surface is generally well-sorted and well-armored. Clasts are either interlocked, partly
761 isolated, and also rooted in a finer-grained matrix, (Figure 6A). At these sites, upper flow
762 regime segments laterally change to lower flow regime reaches over short distances of a
763 few meters (Figure 1B). While we have made this observation during low water stages only,
764 it is likely that sub- and supercritical flows also change during flood stages over short
765 distances, as various examples of Alpine streams show (Spreafico et al., 2001).

767 3.4 Data about clast imbrication from stratigraphic records

768 Here, we calculated patterns of bed roughness and related channel gradients from
769 stratigraphic records and explored c. 50 conglomerate sites for clast imbrication. We used
770 published data about channel depth d , surface gradient S and information about the
771 pattern of the $D_{\beta d}$, which have been reported from the Late Oligocene alluvial megafan
772 conglomerates at Rigi (47°03'N / 8°29'E) and Thun (46°46'N / 7°44'E) situated in the
773 Molasse foreland basin north of the Alpine orogen (Figure 2, Table 1). The depositional
774 evolution of these conglomerates has been related to the rise and the erosion of the Alpine
775 mountain belt (Kempf et al., 1999; Schlunegger and Castelltort, 2016).

776 The Rigi deposits are c. 3600 m thick and made up of an alternation of conglomerates and
777 mudstones (Stürm, 1973) that were deposited between 30 and 25 Ma according to
778 magneto-polarity chronologies and mammal biostratigraphic data (Engesser and Kälin,
779 2017). Garefalakis and Schlunegger (2018) subdivided the Rigi section into four segments
780 labeled as α through δ . The lowermost segments α and β are an alternation of mudstones
781 and conglomerate beds and were deposited by gravelly streams (Stürm, 1973). According
782 to Garefalakis and Schlunegger (2018), the depositional area was characterized by a low
783 surface slope between $0.2 \pm 0.06^\circ$ and $0.4 \pm 0.2^\circ$. Channel depths span the range between
784 1.7 and 2.5 m, and the $D_{\beta d}$ values are between 2 and 6 cm. These measurements result in
785 bed roughness values between 0.02 and 0.05. Except for one site, we found no evidence
786 for imbrication in α and β units (Figures 4, 7A).

787 The top of the Rigi section, referred to as segments γ and δ by Garefalakis and
788 Schlunegger (2018), is an amalgamated stack of conglomerate beds deposited by non-
789 confined braided streams (Stürm, 1973). Garefalakis and Schlunegger (2018) inferred
790 values between $0.65 \pm 0.2^\circ$ and $0.9 \pm 0.4^\circ$ for the palaeo-gradient of the river (Table 1). $D_{\beta d}$
791 values range between 6 and 12 cm, and palaeo-channels were c. 1.2 m deep. This yields
792 a relative bed roughness between c. 0.05 and 0.12. Interestingly, a large number of
793 conglomerate sites within γ and δ display evidence for clast imbrication in outcrops
794 parallel to the palaeo-discharge direction (Figures 4, 6B). In addition, some outcrops show

geo Uni Bern 22.8.2018 10:47

Deleted: where clasts

geo Uni Bern 22.8.2018 10:47

Deleted: , as a photo of a subaquatic longitudinal bar shows

geo Uni Bern 22.8.2018 10:47

Deleted: very

geo Uni Bern 22.8.2018 10:47

Deleted: the occurrence or absence of clast imbrications

geo Uni Bern 22.8.2018 10:47

Deleted: the occurrence or absence of

geo Uni Bern 22.8.2018 10:47

Deleted: imbrications

geo Uni Bern 22.8.2018 10:47

Deleted: gradients

geo Uni Bern 22.8.2018 10:47

Deleted: and the associated erosional history of this orogen

geo Uni Bern 22.8.2018 10:47

Deleted: at Rigi

geo Uni Bern 22.8.2018 10:47

Deleted: this alternation of conglomerates and mudstones

geo Uni Bern 22.8.2018 10:47

Deleted:

geo Uni Bern 22.8.2018 10:47

Deleted: ranging

geo Uni Bern 22.8.2018 10:47

Deleted: imbrications in outcrops of

geo Uni Bern 22.8.2018 10:47

Deleted: these rivers

geo Uni Bern 22.8.2018 10:47

Deleted: the segments

geo Uni Bern 22.8.2018 10:47

Deleted: imbrications

815 sedimentary structures that correspond to cluster bedforms of imbricated clasts (C on
816 Figure 7B). However, at all sites, the lateral extent of these bedforms is limited to 1-2
817 meters. Please refer to Garefalakis and Schlunegger (2018) and their Figure 2 for location
818 of sites displaying units α through δ .

819 The ages of the up to 3000 m-thick Thun conglomerates are younger, and span the time
820 interval between c. 26 and 24 Ma according to magneto-polarity chronologies
821 (Schlunegger et al., 1996). Similar to the Rigi section, the Thun conglomerates start with
822 an alternation of conglomerates, mudstones and sandstones (unit A). This suite is overlain
823 by an up to 2000 m-thick amalgamated stack of conglomerate beds (unit B). Channel
824 depths within unit A range between 3 to 5 m, and streams were between 0.1° and 0.3°
825 steep. Channels in the overlying unit B were shallower and between 1.5 and 3 m deep.
826 Stream gradients varied between 0.4° and 1°, depending on the relationships between
827 inferred water depths and maximum clast sizes (Schlunegger and Norton, 2015). In
828 outcrops parallel to the palaeo-discharge direction, sequences with imbricated clasts have
829 only been found in unit B where palaeo-channel slopes were steeper than 0.4° (Figure 4A).
830 Similar to the Rigi section, the lateral extents of imbricated clasts are limited to a few
831 meters only. No data is available for computing the D_{84} grain size, so that we cannot
832 estimate the bed roughness for the Thun conglomerates. Please refer to Schlunegger and
833 Norton (2015) for location of sites where units A and B are exposed.

834 Similar to the modern examples, imbricated clasts form a well-sorted cluster and
835 commonly include the largest constituents of a gravel bar. In most cases, clasts imbricate
836 behind an outsized constituent, which usually delineates the front of imbricated grains
837 (Figure 7B).

838

839 4 Discussion

840 4.1 Selection of preferred boundary conditions

841 Our calculations reveal that the results strongly dependent on: (i) the selection of values
842 for the Shields variable ϕ ; (ii) the way of how we consider variations in slope S at the bar
843 and reach scales, and (iii) the consideration of flood magnitudes which either result in the
844 motion of individual sediment particles or the change of an entire channel (channel forming
845 floods). This section is devoted to justify the selection of our preferred boundary conditions.

846

847 *Channel forming floods versus onset of grain motion and related thresholds*

848 We constrained our calculations on the incipient motion of individual clasts and used
849 equation (1a) for all other considerations. This might contrast to the hydrological conditions
850 during channel forming floods where thresholds for the evacuation of sediment are up to
851 1.2 times larger, as theoretical and field-based analyses and have shown (Parker, 1978;
852 Philips and Jerolmack, 2016; Pfeiffer et al., 2017). However, a 1.2-times larger threshold
853 will increase the ϕ -values (equation 1b) to the range between 0.036 and 0.072. As

geo Uni Bern 22.8.2018 10:47

Deleted: extents

geo Uni Bern 22.8.2018 10:47

Deleted: groups with imbricated clasts are

geo Uni Bern 22.8.2018 10:47

Deleted: widths of

geo Uni Bern 22.8.2018 10:47

Deleted: at Thun

geo Uni Bern 22.8.2018 10:47

Deleted: slightly

geo Uni Bern 22.8.2018 10:47

Deleted: ,

geo Uni Bern 22.8.2018 10:47

Deleted: the ages

geo Uni Bern 22.8.2018 10:47

Deleted: at Thun

geo Uni Bern 22.8.2018 10:47

Deleted: , which has been referred to as

geo Uni Bern 22.8.2018 10:47

Deleted: .

geo Uni Bern 22.8.2018 10:47

Deleted: groups with

geo Uni Bern 22.8.2018 10:47

Deleted: widths of

geo Uni Bern 22.8.2018 10:47

Deleted: with the consequence

geo Uni Bern 22.8.2018 10:47

Deleted: see

geo Uni Bern 22.8.2018 10:47

Deleted: an

geo Uni Bern 22.8.2018 10:47

Deleted: arrangement of clasts

geo Uni Bern 22.8.2018 10:47

Deleted: are

geo Uni Bern 22.8.2018 10:47

Deleted: alteration of the shape

geo Uni Bern 22.8.2018 10:47

Deleted: Thresholds regarding channel

geo Uni Bern 22.8.2018 10:47

Deleted: incipient

geo Uni Bern 22.8.2018 10:47

Deleted: of individual clasts

geo Uni Bern 22.8.2018 10:47

Deleted: approach

geo Uni Bern 22.8.2018 10:47

Deleted: be perceived as a large

geo Uni Bern 22.8.2018 10:47

Deleted: 20916; Pfeiffer et al., 2017). Nevertheless, the consequences on the outcome of our calculations are minor, at least when the Froude number dependencies on the slope and bed roughness parameters are considered. In fact

geo Uni Bern 22.8.2018 10:47

Deleted: However, as

886 illustrated in Figure 3, this will not change the general pattern. In addition, while channel
887 forming floods, mainly result in the shift of a large range of sediment particles, the formation
888 of an imbricated fabric involves the clustering of individual clasts only. We use these
889 arguments to justify our preference for equation 1a (incipient motion of clasts) rather than
890 equation 1b (channel forming floods).

891

892 *Protrusion and hiding effects and consequences for the selection of ϕ -values*

893 Larger bed surface grains, as is the case for most of the imbricated clasts, may exert lower
894 mobility thresholds because of a greater protrusion and a smaller intergranular friction
895 angle, as noted by Buffington and Montgomery (1997) in their review. This has been
896 explored through experiments and field-based investigations (e.g., Buffington et al., 1992;
897 Johnston et al., 1998). These studies resulted in the notion that the entrainment of the
898 largest clasts (e.g., the D_{84}) requires lower flow strengths than the shift of median-sized
899 sediment particles. Accordingly, while ϕ -values might be as high as 0.1 upon the
900 displacement of the D_{50} (Buffington et al., 1992), conditions for the incipient dislocation of
901 large clasts could be significantly different. In particular, for clasts that are up to five times
902 larger than the D_{50} (which corresponds to the ratio between the D_{84} and the D_{50} of the
903 Swiss data, Table 1), Buffington et al (1992) and also Johnston et al. (1998) predicted ϕ -
904 values that might be as low as 0.03 or even less. Similar ϕ -values, for instance, have
905 indeed been applied for mountain streams where the supply of sediment from the lateral
906 hillslopes has been large (van der Berg and Schlunegger, 2012). This has been
907 considered to result in a poor sorting and a low packing of the material, and thus in low
908 thresholds particularly for the incipient motion of large clast (Lenzi et al., 2006; van der
909 Berg and Schlunegger, 2012). Our calculations predict that an upper flow regime will not
910 establish at these conditions (ϕ -value of 0.03).

911 However, we consider it unlikely that the formation of most of the imbrication, as we did
912 encounter in the analyzed Alpine streams and in the stratigraphic record, was associated
913 with thresholds as low as those proposed by e.g., Lenzi et al. (2006) and van der Berg and
914 Schlunegger (2012). We base our inference on the observation that the large clasts are
915 generally well sorted and densely packed, both on subaerial (during low water stages) and
916 subaquatic bars. This results in a high interlocking degree within the bars we have
917 encountered in the field. In addition, field inspections showed that the base of most of the
918 large clasts, particularly those in subaquatic bars, are embedded and thus buried in finer
919 grained material, and only very few clasts are lying isolated and flat on their a - b -planes.
920 This implies that the fine-grained material has to be removed before these clasts can be
921 entrained. In this case, hiding effects associated with ϕ -values >0.5 would possibly be
922 appropriate for the prediction of material entrainment (Buffington and Montgomery, 1997).
923 Accordingly, a dislocation of the large clasts and thus a rearrangement of the sedimentary

geo Uni Bern 22.8.2018 10:47

Deleted: are

geo Uni Bern 22.8.2018 10:47

Deleted: associated with equal mobility

geo Uni Bern 22.8.2018 10:47

Deleted: using

geo Uni Bern 22.8.2018 10:47

Deleted: Related consequences have

geo Uni Bern 22.8.2018 10:47

Deleted: in

geo Uni Bern 22.8.2018 10:47

Deleted:) and through field-based studies, which were likewise complemented with experiments in the laboratory (

geo Uni Bern 22.8.2018 10:47

Deleted: most likely

geo Uni Bern 22.8.2018 10:47

Deleted: As a consequence

geo Uni Bern 22.8.2018 10:47

Deleted: for

geo Uni Bern 22.8.2018 10:47

Deleted: Related

geo Uni Bern 22.8.2018 10:47

Deleted: mountainous

geo Uni Bern 22.8.2018 10:47

Deleted: Large sediment fluxes have

geo Uni Bern 22.8.2018 10:47

Deleted: is very unlikely to

geo Uni Bern 22.8.2018 10:47

Deleted: imbrications

geo Uni Bern 22.8.2018 10:47

Deleted: were

geo Uni Bern 22.8.2018 10:47

Deleted: analyzed gravel bars display an arrangement where

geo Uni Bern 22.8.2018 10:47

Deleted: of sediment particles

geo Uni Bern 22.8.2018 10:47

Deleted: sediment particles have

geo Uni Bern 22.8.2018 10:47

Deleted: of the finer-grained sediments before the larger clasts can be shifted

geo Uni Bern 22.8.2018 10:47

Deleted: As a consequence

geo Uni Bern 22.8.2018 10:47

Deleted: these

950 fabric most likely requires high-discharge events with large flow strengths, because large
 951 thresholds have to be exceeded. We thus propose that a ϕ -value of c. 0.05, which is
 952 commonly used for the entrainment of the D_{50} (Paola and Moring, 1996), is also adequate
 953 for predicting the hydrological conditions in Alpine streams at the onset of grain motion.
 954 We do acknowledge, however, that this hypothesis warrants a test with quantitative data,
 955 which we have not available. Please note that the low Froude numbers and thus the low ϕ -
 956 values of 0.3 inferred for the Thur and the Birse streams might be underestimates,
 957 because photos taken during high stage flows display clear evidence for multiple hydraulic
 958 jumps over m-long reaches in these streams (Spreafico et al., 2001, p. 71 and 77).

959
 960 *Variations in channel gradient at the bar and reach scales*

961 Figure 3 shows that the results largely hinge on the values of ϕ and S . We applied
 962 equation 3 while inferring a steady uniform flow and a bed slope, which is constant over a
 963 distance of 500 m. We did not consider any smaller-scale slope variations associated with
 964 alternations of bars, riffles and pools as we lack the required quantitative information. Our
 965 simplification results in an energy slope, which is neither equal to the water surface slope
 966 nor to the bed slope. Such inequalities increase substantially when unsteady non-uniform
 967 super-critical flows and transitions are considered (e.g., Figure 1A). This is not fully
 968 described by equations 3 and 4, and thus introduces a bias. Similar variations in bar
 969 morphologies are not depicted in experiments either (e.g., Buffington et al., 1992; Powell et
 970 al., 2016), which could partially explain the low ϕ -values that result from these studies. We
 971 justify our simplification because we are mainly interested in exploring whether
 972 supercritical flows are likely to occur for particular ϕ - and channel gradient values.

973
 974 4.2 Relationships between channel gradient, bed roughness and flow regime

975 We have found an expression where the Froude number F , and thus the change from the
 976 lower to the upper flow regime, depends on the channel gradient S and the bed roughness
 977 D_{Bd}/d (eq. 7). This relationship also predicts that the controls of both parameters on the
 978 Froude number are to some extent independent from each other. Under these
 979 considerations, the similar patterns on Figure 3 are unexpected. However, we note that we
 980 computed both relationships for the case of the incipient motion of the D_{Bd} . This threshold
 981 is explicitly considered by equation 2, which we used as basis to derive an expression
 982 where the Froude number F depends on the channel gradient or the bed roughness only.
 983 Therefore, it is not surprising that the dependency of F on gradient and bed roughness
 984 follows the same trends. In addition, Blissenbach (1952), Paola and Moring (1996) and
 985 also Church (2006) showed that channel gradient, water depth and grain size are closely
 986 related during the entrainment of sediment particles. In particular, channels with coarser
 987 grained gravel bars tend to be steeper and shallower than those where the bed material is

- geo Uni Bern 22.8.2018 10:47
Deleted: require that large thresholds have to be exceeded, which is mainly accomplished through
- geo Uni Bern 22.8.2018 10:47
Deleted: .
- geo Uni Bern 22.8.2018 10:47
Deleted: the use of ϕ -values
- geo Uni Bern 22.8.2018 10:47
Deleted: the calculation of
- geo Uni Bern 22.8.2018 10:47
Deleted: associated with the fabric we have encountered
- geo Uni Bern 22.8.2018 10:47
Deleted: the field
- geo Uni Bern 22.8.2018 10:47
Deleted: underestimated
- geo Uni Bern 22.8.2018 10:47
Deleted: that were
- geo Uni Bern 22.8.2018 10:47
Deleted: of these streams
- geo Uni Bern 22.8.2018 10:47
Deleted: that are caused by downstream
- geo Uni Bern 22.8.2018 10:47
Deleted: This inference
- geo Uni Bern 22.8.2018 10:47
Deleted:), which
- geo Uni Bern 22.8.2018 10:47
Deleted: ,
- geo Uni Bern 22.8.2018 10:47
Deleted: which
- geo Uni Bern 22.8.2018 10:47
Deleted: These
- geo Uni Bern 22.8.2018 10:47
Deleted: channel floor
- geo Uni Bern 22.8.2018 10:47
Deleted: likewise
- geo Uni Bern 22.8.2018 10:47
Deleted: pattern of how the Froude number F depends
- geo Uni Bern 22.8.2018 10:47
Deleted: channel gradient and bed roughness (
- geo Uni Bern 22.8.2018 10:47
Deleted:) appears
- geo Uni Bern 22.8.2018 10:47
Deleted: grain size percentile
- geo Uni Bern 22.8.2018 10:47
Deleted: dependencies
- geo Uni Bern 22.8.2018 10:47
Deleted: the Froude number
- geo Uni Bern 22.8.2018 10:47
Deleted: follow
- geo Uni Bern 22.8.2018 10:47
Deleted: parameters

1018 finer grained (Church, 2006). In the same sense, bed roughness tends to be larger in
1019 steeper streams than in flatter channels (Whipple, 2004). We use the causal relationships
1020 between these variables to explain the similarities in Figures 3A and 3B.

geo Uni Bern 22.8.2018 10:47
Deleted: also in steeper streams, ... [24]

1021 The tendency towards lower Froude numbers for a channel gradient $>1^\circ$ ($\phi >0.05$) and a
1022 bed roughness >0.3 ($\phi >0.05$) is somewhat unexpected. We explain these trends through
1023 the non-linear relationships between slope, water depth, the energy loss within the
1024 roughness-layer, and the velocity at the flow's surface.

1025

1026 4.3 The formation of imbrication in experiments

1027 Interpretations of the possible linkages between hydrological conditions upon material
1028 transport and the formation of imbrication are hampered because experiments have not
1029 been designed to explicitly explore these relationships. In addition, as noted by Carling et
1030 al. (1992), natural systems differ from experiments because of the contrasts in scales.

geo Uni Bern 22.8.2018 10:47
Deleted: imbrications

1031 Nevertheless, many experiments have reproduced clast imbrication in subcritical flumes
1032 (Carling et al., 1992) or even in stationary flows (Aberle and Nikora, 2006). For instance,
1033 imbrication was reproduced at low Froude numbers between c. 0.55 and 0.9 (Powell et al.,
1034 2016; Bertin and Friedrich, 2018), or at least during some non-specified subcritical flow
1035 (Johansson, 1963). Note that we inferred the Froude numbers from the experimental setup
1036 of these authors. Also in experiments, material transport occurred at ϕ -values as low as
1037 0.03 (Powell et al., 2016), which is consistent with the low Froude numbers for some of the
1038 streams in Switzerland. Based on field observations, Sengupta (1966) reported examples
1039 where pebbles embedded in sand formed started to imbricate during lower regime flows. In
1040 these examples, eddies developed at the upstream end of pebbles, which then lead to the
1041 winnowing of the fine-grained sand at the upstream edge and the tilting of this particular
1042 clast. Additional sliding, pivoting and vibrating of these sediment particles then resulted in
1043 the final imbrication. If this process occurs multiple times and affects the sand-gravel
1044 interface at various sites, then an armored bed with imbricated clasts can establish without
1045 the necessity of supercritical flows, or changes in flow regimes, as experimental results
1046 have shown (Aberle and Nikora, 2006; Haynes and Pender, 2007). Such a fabric may
1047 even form in response to prolonged periods of sub-threshold flows, as summarized by
1048 Ockelford and Haynes (2013). Also through flume experiments in a 0.3 m-wide, 4 m-long,
1049 recirculating tilting channel flume, Brayshaw (1984) was able to reproduce cluster
1050 bedforms with imbricated clasts during subcritical flows (F -numbers between 0.03 and
1051 0.07). In addition to these complexities, Carling et al. (1992) showed that the shape of a
1052 clast has a strong control on the thresholds for incipient motion, the style of motion, and
1053 the degree of imbrication.

geo Uni Bern 22.8.2018 10:47
Deleted: imbrications...mbricator ... [25]

1054 However, inspections of photos illustrating the experimental set up reveal that the surface
1055 grains are either flat lying on finer-grained sediments before their entrainment (Figure 3 in

1114 Powell et al., 2016), occur isolated on the ground (Figure 2.1b in Carling et al., 1992), or
1115 have a low degree of interlocking (Figure 3a in Lamb et al., 2017). Interestingly, the
1116 experiment by Buffington et al. (1992) followed a different strategy, where a natural bed-
1117 surface of a stream was peeled off with epoxy. They subsequently used this peel in the
1118 laboratory to approximate a natural channel bed surface (see their Figure 4), on top of
1119 which they randomly placed grains with a known size distribution. Buffington and co-
1120 authors then measured the friction angle of the overlying grains, based on which they
1121 calculated the critical boundary shear stress values ϕ . In all experiments, the surface
1122 morphology lacks topographic variations, which we found as reach-scale alternations of
1123 riffles, transverse bars and pools in the field. The low ϕ -values of 0.03, which appears to
1124 be typical of bed surfaces in laboratory flumes (Ferguson, 2012), as summarized by Powell
1125 et al. (2016), could possibly be explained by these conditions. Furthermore, and probably
1126 more relevant, the experimental reaches are quite short in comparison to natural settings
1127 and range between e.g., 4.0 meters (Brayshaw, 1984), 4.4 meters (Powell et al., 2016), 15
1128 meters (e.g., Lamb et al., 2017) and 20 meters (Aberle and Nikora, 2006). We
1129 acknowledge that in most experiments the variables have been normalized through an e.g.,
1130 constant Reynolds or Froude number (Brayshaw, 1984). This normalization also includes
1131 the experimental D_{50} -grain sizes, which are very similar to those of our streams (Litty and
1132 Schlunegger, 2017). Nevertheless, we find it really hard to upscale some of the
1133 experimental results to our natural cases where standing waves of 1 m, and even between
1134 5 and 8 meters lengths may occur (our Figures 1B, 5B, 6B, supplement), which are not
1135 reproducible in experiments. In addition, Powell et al. (2016) observed that the water
1136 surface stayed relatively stable during their experiments, and that the flows were steady
1137 and uniform without hydraulic jumps. This contrasts to our natural cases where upper and
1138 lower flow regimes alternate over short distances even during low-stage flows. Finally,
1139 while winnowing of fine-grained material, tilting and imbrication of clasts and subsequent
1140 bed armoring might be valuable mechanisms during subcritical flows in experiments, we
1141 consider it unlikely that this can be directly translated to our field observations. We base
1142 our inference on two closely related arguments. First, our reported groups of imbricated
1143 clasts tend to be arranged as cluster bedforms (e.g., Figures 6D, 7B), which rather form in
1144 response to selective deposition of large clasts (Brayshaw, 1984) than selective
1145 entrainment of fine-grained material (Figure 6A). Second, observations (Berther, 2012) and
1146 calculations (Litty and Schlunegger, 2017) have shown that effective sediment transport in
1147 these streams is likely to occur on decadal time scales (and most likely much shorter; van
1148 der Berg and Schlunegger, 2012), at least for subaquatic bars. Sediment transport is then
1149 likely to occur over a limited reach only. This means that a large fraction of the shifted
1150 material per flood has a local source situated in the same river some hundreds of meters
1151 farther upstream where bars are also well armored. This possibly calls for large thresholds
1152 for the removal of clasts. In addition, on subaerial bars, fine-grained material is deposited

geo Uni Bern 22.8.2018 10:47
Deleted: of the sedimentary material is flat and

geo Uni Bern 22.8.2018 10:47
Deleted: surface conditions that develop

geo Uni Bern 22.8.2018 10:47
Deleted: lengths of the

geo Uni Bern 22.8.2018 10:47
Deleted: generally less

geo Uni Bern 22.8.2018 10:47
Deleted: even

geo Uni Bern 22.8.2018 10:47
Deleted: we have determined for

geo Uni Bern 22.8.2018 10:47
Deleted: selected

geo Uni Bern 22.8.2018 10:47
Deleted: associated with these experiments

geo Uni Bern 22.8.2018 10:47
Deleted: the

geo Uni Bern 22.8.2018 10:47
Deleted:

geo Uni Bern 22.8.2018 10:47
Deleted: armoring

geo Uni Bern 22.8.2018 10:47
Deleted: a

geo Uni Bern 22.8.2018 10:47
Deleted: mechanism for the explanation of imbrications

geo Uni Bern 22.8.2018 10:47
Deleted: low stage

geo Uni Bern 22.8.2018 10:47
Deleted: these results

geo Uni Bern 22.8.2018 10:47
Deleted: waning stages of floods result in the deposition of

1173 | and not winnowed during waning stages of floods, as our observations have shown.
1174 | Accordingly, while low ϕ -values and thus a lower flow regime might be appropriate for
1175 | predicting the entrainment of sediment particles in experiments, greater thresholds and
1176 | thus larger ϕ -values are likely to be appropriate for our natural examples for the reasons
1177 | we have explained above.

geo Uni Bern 22.8.2018 10:47
Deleted: in the winnowing of ... [26]

1178 |

1179 | 4.4 Relationships between flow regime and clast imbrication in the field

1180 | Here, we provide evidence for linking clast imbrication with supercritical flows provided that
1181 | gravels are well-sorted and densely packed and form a clast-supported fabric. We sustain
1182 | our inferences with (i) published examples from natural environments; (ii) our observations
1183 | from Swiss streams; and (iii) the results of our calculations,

geo Uni Bern 22.8.2018 10:47
Deleted: Possible ... [27]

geo Uni Bern 22.8.2018 10:47
Deleted: proposing that...inking c... [28]

1184 | For the North Saskatchewan River in Canada, Shaw and Kellerhals (1977) reported gravel
1185 | mounds on a lateral gravel bar with a spacing between 2 and 3 meters and a relatively flat
1186 | top. Shaw and Kellerhals considered these bedforms as antidunes, which might have
1187 | formed in the upper flow regime. In the same sense, transverse ribs were considered as

geo Uni Bern 22.8.2018 10:47
Deleted: , which have a regular... [29]

1188 | evidence for the deposition either under upper flow regime conditions, or in response to
1189 | upstream-migrating hydraulic jumps (e.g., Koster, 1978; Rust and Gostin, 1981). These
1190 | features have been described from modern streams as a series of narrow, current-
1191 | normally orientated accumulations of large clasts. Koster (1978) additionally reported that

geo Uni Bern 22.8.2018 10:47
Formatted: Font color: Auto, Pattern: Clear

1192 | transverse ribs are associated with clast imbrication (Figure 2 in Koster, 1978). Alexander
1193 | and Fielding (1997) found modern gravel antidunes with well-developed clast imbrication in
1194 | the Burdekin River, Australia. Finally, Taki and Parker (2005) reported cyclic steps of
1195 | channel floor bedforms with wave-lengths 100–500 times larger than the flow thickness.

geo Uni Bern 22.8.2018 10:47
Deleted: these bedforms

geo Uni Bern 22.8.2018 10:47
Deleted: imbrications...mbricator... [30]

1196 | These bedforms most likely represent chute-and-pool configurations (Taki and Parker,
1197 | 2005), which could have formed in response to alternations of upper and lower flow regime
1198 | conditions, as outlined by Grant (1997). In such a situation, the upstream flow on the
1199 | stoss-side of the bedform experiences a reduction of the flow velocity, with the effect that

geo Uni Bern 22.8.2018 10:47
Formatted: Font color: Auto, Pattern: Clear

1200 | the flow may shift to subcritical conditions. This would be associated with a hydraulic jump
1201 | and a flow velocity reduction and thus with a drop of shear stresses (Figure 1A), which
1202 | could result in the deposition of clasts. In such a scenario, the site of sediment
1203 | accumulation most likely migrates upstream (Figure 8).

1204 | Our inspections of modern gravel bars and stratigraphic records (Figure 4) reveal the
1205 | occurrence of imbrication where channel slopes are steeper than 0.4° - 0.5° , and where the
1206 | values of bed roughness exceed c. 0.06. The results of our generic calculations (Figure 3)
1207 | reveal that flows might become supercritical under these conditions, provided ϕ is greater
1208 | than c. 0.05 (Figure 3). This is supported by observations from the Waldemme and Reuss

geo Uni Bern 22.8.2018 10:47
Deleted: Inspections...ur inspecti... [31]

1209 | Rivers (slope $>0.5^{\circ}$) during high and low stage flows (Figures 5B and 6B) that provide
1210 | evidence for standing waves and thus supercritical flows (supplement). Contrariwise, the

1256 reach of the Emme River is flatter (slope $<0.4^\circ$), imbrication is largely absent, and flows
1257 are generally subcritical (Spreafico et al., 2001, p. 53). We thus propose that a channel
1258 gradient of c. 0.5° is critical for both the formation of clast imbrication and possibly also for
1259 the establishment of supercritical flows. Based on these relationships, we suggest that the
1260 generation of imbrication occurs at upper flow regime conditions.

1261 The proposed threshold slope is consistent with the results of previous work, where upper
1262 flow regime bedforms such as transvers ribs have been described for e.g., the Peyto
1263 Outwash (slope c. 1.09°), the Spring Creek (same slope; McDonald and Banerjee, 1971),
1264 and the North Saskatchewan River (slope 0.52° ; Dept. Mines and Tech. Survs., 1957).
1265 This is also in agreement with observations (Mueller et al., 2005) and the results of
1266 theoretical work calibrated with data (Lamb et al., 2008). In particular, Mueller et al. (2005)
1267 suggested that a ϕ -value of c. 0.03 is suitable for slopes $<0.35^\circ$, while $\phi > 0.1$ might be
1268 more appropriate for the mobilization of coarse-grained material in channels steeper than
1269 1.1° . This might be an overestimate of the ϕ -dependency of slope (Lamb et al., 2008), but
1270 it does show that ϕ -values larger than 0.04 and 0.05 might be appropriate where channels
1271 are steep (see also Ferguson, 2012). Finally, Simons and Richardson (1960, p. 45) noted
1272 that flows rarely exceed unity Froude numbers over an extended period of time in a stream
1273 with erodible banks. We thus use the conclusion of these authors to explain the limited
1274 spatial extent of imbricated clasts in modern streams and stratigraphic records.

1275 5 Summary and conclusions

1276 We started with the hypothesis that the transport and deposition of coarse-grained
1277 particles, and particularly the formation of an imbricated fabric, may be related to changes
1278 in flow regimes. We then calculated the Froude number F at conditions of incipient motion
1279 of coarse-grained bedload for various bed roughness and stream gradient values, and we
1280 compared the results with data from modern streams and stratigraphic records. The results
1281 suggest that imbrication is likely to provide evidence for supercritical conditions particularly
1282 where channels are steeper than $\sim 0.5^\circ$ and where ϕ -values are greater than c. 0.05. We
1283 do acknowledge that our field-based inferences are associated with large uncertainties
1284 regarding channel gradients and grain size (Litty and Schlunegger, 2017), and that they
1285 lack a quantitative measure of the spatial distribution of clast imbrication (Bertin and
1286 Friedrich, 2018). In the same sense, our hydrologic calculations are based on the simplest
1287 published relationships between water flow and sediment transport. Greater complexities,
1288 about material transport (Engelund and Hansen, 1967) have not been considered. This
1289 includes, for instance, large supply rates of sediment (van der Berg and Schlunegger,
1290 2012; Bekaddour et al., 2013), changes in bed morphology, spatial variations in
1291 turbulences, the shape and the sorting of grains, the 3D arrangement of clasts (Lamb et al.,
1292 2008; Hodge et al., 2009), and complex hydrological conditions including upper-stage plain

geo Uni Bern 22.8.2018 10:47

Deleted: imbrications are

geo Uni Bern 22.8.2018 10:47

Deleted: occur in the lower flow regime

geo Uni Bern 22.8.2018 10:47

Deleted: imbrications

geo Uni Bern 22.8.2018 10:47

Deleted: also

geo Uni Bern 22.8.2018 10:47

Deleted: imbrications may be associated with

geo Uni Bern 22.8.2018 10:47

Deleted: sediment particles

geo Uni Bern 22.8.2018 10:47

Deleted: the commonly used ϕ -values between 0.04 and 0.05

geo Uni Bern 22.8.2018 10:47

Deleted: exceeded

geo Uni Bern 22.8.2018 10:47

Deleted: their discussion

geo Uni Bern 22.8.2018 10:47

Deleted: of individual ensembles

geo Uni Bern 22.8.2018 10:47

Deleted: imbricated clasts are

geo Uni Bern 22.8.2018 10:47

Deleted: the occurrence of

geo Uni Bern 22.8.2018 10:47

Deleted: at sites

geo Uni Bern 22.8.2018 10:47

Deleted: channel gradients

geo Uni Bern 22.8.2018 10:47

Deleted: imbrications and clast arrangements

geo Uni Bern 22.8.2018 10:47

Deleted: the

geo Uni Bern 22.8.2018 10:47

Deleted: and force balancing approaches

geo Uni Bern 22.8.2018 10:47

Deleted: expressions where

geo Uni Bern 22.8.2018 10:47

Deleted: is related to

geo Uni Bern 22.8.2018 10:47

Deleted: Larger

geo Uni Bern 22.8.2018 10:47

Deleted: , which complicate any considerations of

geo Uni Bern 22.8.2018 10:47

Deleted:),

geo Uni Bern 22.8.2018 10:47

Deleted: more

1322 beds, hydraulic drops, and standing waves (Johannson, 1963). In addition, the occurrence
1323 or absence of imbrication also depends on the shape of the involved clasts (Carling et al.,
1324 1992), where a relatively large c-axis tends to form a steeper imbrication compared to a
1325 short c-axis. In addition, experiments showed that spheres and rods have a higher mobility
1326 than blades and discs (Hattinigh and Illenberger, 1995). Unfortunately, we lack the
1327 quantitative dataset to properly address these points. We also acknowledge that
1328 imbrication is formed in experiments under subcritical flows with low ϕ -values (Brayshaw,
1329 1984; Carling et al., 1992; Powell et al., 2016; Lamb et al., 2017). However, as already
1330 noted above, we find it quite hard to upscale the experimental results (<20 meters) to the
1331 reach scale of our observations where standing waves with wavelengths as long as 8
1332 meters have been observed (Figure 6B, supplement).

1333 Despite our simplifications, we find evidence for proposing that the formation of imbrication
1334 likely occurs at supercritical conditions provided that (i) channels are steeper than c.
1335 $0.5^\circ \pm 0.1^\circ$, and (ii) large clasts are tightly packed, closely arranged as cluster bedforms and
1336 partly embedded in finer-grained sediment. Mobilization and rearrangement of these
1337 structures require greater thresholds (Brayshaw, 1985), which might be large enough
1338 (ϕ -values possibly >0.05) to allow supercritical conditions to occur. These findings might
1339 be useful for the quantification of hydrological conditions recorded in the stratigraphic
1340 record such as conglomerates. As a further implication, the occurrence of imbrication in
1341 geological archives may be used to infer a minimum palaeo-topographic slope of $0.5^\circ \pm 0.1^\circ$
1342 at the time the sediments were deposited. Such a constraint might be beneficial for palaeo-
1343 geographic reconstructions and for the subsidence analysis of sedimentary basins (e.g.,
1344 Schlunegger et al., 1997). Finally, for modern streams, the presence of imbrication on
1345 gravel bars might be more conclusive for inferring an upper flow regime upon material
1346 transport than other bedforms such as transverse ribs or antidunes (Koster, 1978; Rust
1347 and Gostin, 1981), mainly because clast imbrication has a better preservation potential
1348 and is easier to recognize in the field.

1349

1350 Figure captions

1351 Figure 1: A) Photo showing hydraulic jump, and conceptualization of situation displayed
1352 in photo of Figure 1A. F =Froude number; v =flow velocity, d =water depth. B)
1353 Photo from Sense River, and cross-sections through reaches with upper and
1354 lower flow regimes. Surface waves ($\lambda \approx 20$ -30 cm) tend to fade out towards the
1355 upstream direction relative to the flow movement where subcritical flows prevail
1356 (section to the left). A hydraulic jump separates supercritical from subcritical
1357 flow where the bedrock builds a ramp. The reach illustrated by the section to
1358 the right is characterized by standing waves with wavelengths $\lambda \approx 100$ cm. The

geo Uni Bern 22.8.2018 10:47

Deleted: imbrications...mbrication ... [32]

geo Uni Bern 22.8.2018 10:47

Deleted: clast imbrications are... [33]

geo Uni Bern 22.8.2018 10:47

Deleted: segments with a ... [34]

1400 dashed line illustrates the trace of the plane that separates lower from upper
1401 regime flows. Please see Figure 2 for location of photo.

1402

1403 Figure 2: Sites where modern gravel bars in streams were inspected for the occurrence
1404 of clast **imbrication** (blue dots). The figure also shows the locations of the
1405 stratigraphic sections where conglomerates were analyzed for their
1406 sedimentary structures. S=Sense; E=Emme; WE_{L/V}=Waldemme,
1407 WL=Waldemme at Littau, R=Reuss; L=Landquart; G=Glener; M_B, M_V,
1408 M_L=Maggia at Bignasco, Visletto and Losone; V_F, V_M, V_L=Verzasca at Frasco,
1409 Motta and Lavertezzo. See Table 1 for coordinates of sites.

1410 The black squares are sites where Spreafico et al. (2001) have estimated
1411 channel gradients and Froude numbers for low and high-stage flows. *b*=Birse-
1412 Moutier, *e*=Emme-Burgdorf, *gl*=Glatt-Fällanden, *g*=Gürbe-Belp, *m*=Minster-
1413 Euthal, *l*=Lütschine-Gsteig, *s*=Suze-Sonceboz, *t*=Thur-Stein

1414

1415 Figure 3: Relationships between A) channel slope and Froude number *F*, and B) relative
1416 bed roughness and *F*. These were calculated as a function of various Shields
1417 (1936) variables ϕ . The pale green field indicates the conditions where an
1418 upper flow regime could prevail, while the yellow field delineates the
1419 occurrence of lower flow regime conditions. In this context, we set the
1420 threshold to a Froude number of c. 0.9. This is consistent with the estimation of
1421 parameters for the formation of upper flow regime bedforms by Koster (1978).
1422 Note that the bed roughness is the ratio between the $D_{\beta d}$ and the water depth *d*
1423 at the **onset of** motion of that particular size class. The vertical bars on Figure
1424 3A also illustrate the Froude numbers that have been estimated by Spreafico
1425 et al. (2001) for the following streams and locations: *b*=Birse-Moutier,
1426 *e*=Emme-Burgdorf, *gl*=Glatt-Fällanden, *g*=Gürbe-Belp, *m*=Minster-Euthal,
1427 *l*=Lütschine-Gsteig, *s*=Suze-Sonceboz, *t*=Thur-Stein. Please note that the low
1428 values for the Thur and Birse Rivers might represent underestimates as these
1429 streams show evidence for multiple hydraulic jumps during high stage flows.

1430

1431 Figure 4: This figure relates the occurrence of **imbrication** (blue bars) or no **imbrication**
1432 (red bars) to A) channel slopes and B) relative bed roughness. Red bars with
1433 blue hatches indicate that **imbrication has** been found in places. Blue bars with
1434 red hatches suggest that **imbrication** dominate the bar morphology, but that
1435 reaches without **imbrication** are also present on the same gravel bar. Data from
1436 modern streams are displayed above the horizontal axes, while information
1437 from stratigraphic sections are placed below the slope and roughness axes,
1438 respectively. S=Sense, S'=Sense with bedrock reach, E=Emme, WE_L,

geo Uni Bern 22.8.2018 10:47
Deleted: imbrications

geo Uni Bern 22.8.2018 10:47
Deleted: incipient

geo Uni Bern 22.8.2018 10:47
Deleted: imbrications

geo Uni Bern 22.8.2018 10:47
Deleted: imbrications

geo Uni Bern 22.8.2018 10:47
Deleted: imbrications have

geo Uni Bern 22.8.2018 10:47
Deleted: imbrications

geo Uni Bern 22.8.2018 10:47
Deleted: imbrications

1446 W =Waldemme, WL =Waldemme at Littau, R =Reuss; L =Landquart; G =Glenner;
1447 M_B , M_V , M_L =Maggia at Bignasco, Visletto and Losone; V_F , V_M , V_L =Verzasca at
1448 Frasco, Motta and Lavertezzo. See Table 1 for coordinates of sites, and Figure
1449 2 for locations where data were collected.

1450

1451 Figure 5 A) Reuss River with evidence for standing waves along the thalweg. Othophoto
1452 reproduced by permission of swisstopo (BA 18065). Please see Figure 2 for
1453 location. B) Transverse and lateral bars in the Reuss River with imbricated
1454 clasts on the lateral bar forming a riffle, and standing waves where the thalweg
1455 crosses the riffle. The wavelength of the standing wave is c. 5 m. Arrow
1456 indicates flow direction. Please see Figures 2 and 5A for location of photo.

1457

1458 Figure 6: Photos from the field. A) Photo of subaquatic longitudinal bar taken along the
1459 steep bedrock/gravel bar reach of the Sense River (see Figure 1B for location
1460 of photo). The clasts in the foreground are clustered and imbricated, forming
1461 the nucleus of a possible cluster bedform. This fabric most likely formed when
1462 rolling clasts came to a halt behind the boulder at the front. The clasts in the
1463 background are either flat lying or slightly imbricated. Except for a few sites,
1464 nearly all grains are either partially buried by finer grained material or
1465 interlocked by neighboring clasts. The overlying flow shows evidence for
1466 supercritical conditions with standing waves. B) Standing waves with a
1467 wavelength of c. 8 m in the Waldemme at Littau. Water fluxes are c. 100 m³/s.
1468 Arrow indicates flow direction. [See also supplement.](#) C) Flat lying clasts on a
1469 lateral bar in the Sense River. Arrow indicates clasts that are overlapping each
1470 other, resulting in a shallow dip of <10° of the overriding clast. D) Imbricated
1471 clasts within the Maggia River at Visletto. Arrow indicates flow direction. Please
1472 note that the imbricated arrangements of clasts mainly include the largest
1473 constituents of the gravel bar in the middle of the photo, and clasts of similar
1474 sizes. Therefore, for this set of imbricated clasts, we do not consider that
1475 protrusion effects might play a major role. See Figure 2 for location and Table
1476 1 for coordinates.

1477

1478 Figure 7: A) Conglomerates at Rigi with no evidence for clast ~~imbrication~~. White lines
1479 indicate the orientation of the bedding. B) Conglomerates at Rigi with
1480 imbricated gravels to cobbles that are arranged as cluster bedforms (C). Arrow
1481 indicates palaeoflow direction. White line refers to the bedding. Note that the
1482 steep dip (>25°) of the *a-b*-planes of the imbricated clasts. See Figure 2 for
1483 location and Table 1 for coordinates.

1484

geo Uni Bern 22.8.2018 10:47
Deleted: imbrications

1486 Figure 8: Conceptual sketch illustrating the formation of an ensemble of imbricated
1487 clasts as time proceeds (A through C). According to this model, the site of
1488 sediment accumulation will migrate upstream. F =Froude number; v =flow
1489 velocity, d =water depth.

1490

1491 Table 1: Grain size and observational data and that have been collected in the field.
1492 See text for further explanations.

1493

1494

1495 **Author contribution**

1496 FS designed the study and carried out the calculations, PG and FS collected the data, FS
1497 wrote the text with contributions by PG, both authors contributed to the analyses and
1498 discussion of the results.

1499

1500 **Data availability**

1501 The authors declare they have no conflict of interest.

1502

1503 **Acknowledgements**

1504 This research has been supported grant No 154198 awarded to Schlunegger by the Swiss
1505 National Science Foundation.

1506

1507 **References**

1508 Aberle, J., and Nikora, V., Statistical properties of armored gravel bed surfaces, *Water*
1509 *Resour. Res.*, 42, W11414, 2006.

1510 Allen, P.A., *Earth Surface Processes*, John Wiley and Sons, Oxford, 416 pp., 1997.

1511 Andrews, E.D., Bed-material entrainment and hydraulic geometry of gravel-bed rivers
1512 in Colorado, *GSA Bull.*, 95, 371-378, 1984.

1513 Alexander, J., Bridge, J.S., Cheel, R.J., and Leclair, S.F., Bedforms and associated
1514 sedimentary structures formed under supercritical water flows over aggrading
1515 sand beds, *Sedimentology*, 48, 133-152, 2001.

1516 Alexander, J., and Fielding, C., Gravel antidunes in the tropical Burdekin River,
1517 Queensland, Australia, *Sedimentology*, 44, 327-337, 1997.

1518 Berther, R., *Geomorphometrische Untersuchungen entlang der Entle*, Ms. Thesis, Univ.
1519 Bern, Bern, Switzerland, 94 p., 2012.

1520 Blissenbach, L., Relation of surface angle distribution to particle size distribution on
1521 alluvial fans, *J. Sediment. Petrol.*, 22, 25-28, 1952.

1522 Bekaddour, T., Schlunegger, F., Attal, M., and Norton, P.K., Lateral sediment sources
1523 and knickzones as controls on spatio-temporal variations of sediment transport
1524 in an Alpine river, *Sedimentology*, 60, 342-357, 2013.

1525 Bray, D.I., and Church, M., Armored versus paved gravel beds. J. Hydraul. Div., 106,
1526 1937-1940, 1980.

1527 Buffington, J., Dietrich, W.E., and Kirchner, J.W., Friction angle measurements on a
1528 naturally formed gravel streambed: Implications for critical boundary shear
1529 stress, Water Res. Res., 28, 411-425, 1992.

1530 Buffington, J.M., and Montgomery, D. R., A systematic analysis of eight decades of
1531 incipient motion studies, with special reference to gravel-bedded rivers, Water
1532 Resour. Res., 33, 1993-2029, 1997.

1533 Bertin, S., and Friedrich, H., Effect of surface texture and structure on the development
1534 of stable fluvial armors, Geomorphology, 306, 64-79, 2018.

1535 Brayshaw, A.C., Characteristics and origin of cluster bedforms in coarse-grained
1536 alluvial channels, in: Sedimentology of Gravels and Conglomerates, edited by
1537 Koster, E.H., and Steel, R.J., Mem. Can. Soc. Petrol. Geol., 10, 77-85, 1984.,
1538 1978.

1539 Brayshaw, A.C., Bed microtopography and entrainment thresholds in gravel-bed rivers,
1540 GSA Bull., 96, 218-223, 1985.

1541 D'Arcy, M., Roda-Boluda, D.C., and Whittaker, A.C., Glacial-interglacial climate
1542 changes recorded by debris flow fan deposits, Owens Valley, California, Quat.
1543 Sci. Rev., 169, 288-311, 2017.

1544 Carling, P.A., Armored versus paved gravel beds – discussion. J. Hydraul. Div., 107,
1545 1117-1118, 1981.

1546 Carling, P.A., Kelsey, A., and Glaister, M.S., Effect of bed roughness, particle shape
1547 and orientation on initial motion criteria, in: Dynamics of gravel-bed rivers,
1548 edited by: Billi, P., Hey, R.D., Throne, C.R., and Tacconi, P., 23-39. John Wiley
1549 and Sons, Ltd., Chichester, 1992.

1550 Church, M., Palaeohydrological reconstructions from a Holocene valley fill, Fluvial
1551 sedimentology, edited by: Miall, A.D., Mem. Can. Soc. Petrol. Geol., 5, 743-772,
1552 1978.

1553 Church, M., Bed material transport and the morphology of alluvial river channels, Ann.
1554 Rev. Earth Planet. Sci., 34, 325–354, 2006.

1555 Department of Mines and Technology Surveys, Atlas of Canada, Geogr. Branch,
1556 Ottawa, 1957.

1557 Duller, R.A., Whittaker, A.C., Swinehart, J.B., Armitage, J.J., Sinclair, H.D., Bair, A.,
1558 and Allen, P.A., Abrupt landscape change post-6Ma on the central Great Plains,
1559 USA, Geology, 40, 871-874, 2012.

1560 Engesser, B., and Kälin, D., *Eomys helveticus* n. sp. and *Eomys schluneggeri* n. sp.,
1561 two new small eomyids of the Chattian (MP 25/MP 26) subalpine Lower
1562 Freshwater Molasse of Switzerland, Fossil Imprint, 73, 213–224, 2017.

1563 Engelund, F., and Hansen, E., A monograph on sediment transport in alluvial streams,
1564 Teknisk Forlag – Copenhagen, 62 pp., 1967.

1565 Ferguson, R., Flow resistance equations for gravel- and boulder- bed streams. *Water*
1566 *Resour. Res.*, 43, W05427, 2007.

1567 Ferguson, R., River channel slope, flow resistance, and gravel entrainment thresholds,
1568 *Water Resour. Res.*, 48, W05517, doi:10.1029/2011WR010850, 2012.

1569 Garefalakis, P., and Schlunegger, F., Link between concentrations of sediment flux and
1570 deep crustal processes beneath the European Alps, *Sci. Rep.*, 8, 183,
1571 doi:10.1038/s41598-017-17182-8

1572 Grant, G.E., Swanson, F.J., and Wolman, M.G., Pattern and origin of stepped-bed
1573 morphology in high gradient streams, western Cascades, Oregon, *GSA Bull.*, 102,
1574 340–352, 1990.

1575 Grant, G.E., Critical flow constrains flow hydraulics in mobile-bed streams: A new
1576 hypothesis, *Water Resour. Res.*, 33, 349-358, 1997.

1577 Haynes, H., and Pender, G., Stress history effects on graded bed stability, *J. Hydraul.*
1578 *Eng.*, 33, 343-349, 2007.

1579 Hattingh, J., and Illenberger, W.K., Shape sorting of flood-transported synthetic clasts
1580 in a gravel bed river, *Sed. Geol.*, 96, 181-190, 1995.

1581 Hey, R.D., and Thorne, C.R., Stable channels with mobile gravel beds, *J. Hydr. Eng.*,
1582 112, 671-689, 1986.

1583 Hodge, R., Brasington, J., and Richards, K., In situ characterization of grain-scale
1584 fluvial morphology using Terrestrial Laser Scanning, *Earth Surf. Process.*
1585 *Landf.*, 34, 954-968, 2009.

1586 Howard, A.D., in: *Thresholds in Geomorphology*, edited by: Coates, D.R., and Vitek,
1587 J.D., Allen and Unwin, Boston, MA, 227-258, 1980.

1588 Jarrett, R.D., Hydraulics of high-gradient streams. *J. Hydr. Eng.*, 110, 1519-1939,
1589 1984.

1590 Johansson, C.E., Orientation of pebbles in running water: a laboratory study, *Geogr.*
1591 *Ann.*, 45, 85-112, 1963.

1592 Johnston, C.E., Andrews, E.D., and Pitlick, J., In situ determination of particle friction
1593 angles of fluvial gravels, *Water Resour. Res.*, 34, 2017-2030, 1998.

1594 Kempf, O., Matter, A., Burbank, D.W., and Mange, M., Depositional and structural
1595 evolution of a foreland basin margin in a magnetostratigraphic framework; the
1596 eastern Swiss Molasse Basin, *Int. J. Earth Sci.*, 88, 253–275, 1999.

1597 Kirchner, J.W., Dietrich, W.E., Iseya, F., and Ikeda, H., The variability of critical shear
1598 stress, friction angle, and grain protrusion in water-worked sediments,
1599 *Sedimentology*, 37, 647-672, 1990.

1600 Koster, E.H., Transverse ribs: their characteristics, origin and paleohydraulic
 1601 significance, in: *Fluvial sedimentology*, edited by: Miall, A.D., Mem. Can. Soc.
 1602 Petrol. Geol., 5, 161-186, 1978.

1603 Krogstad, P.A., and Antonia, R.A., Surface roughness effects in turbulent boundary
 1604 layers, *Exp. Fluids*, 27, 450-460, 1999.

1605 Lamb, M.P., Dietrich, W.E., and Venditti, J.G., Is the critical Shields stress for incipient
 1606 sediment motion dependent on channel bed slope?, *J. Geophys. Res.*, 113,
 1607 F02008, 2008.

1608 Lamb, M.P., Brun, F., and Fuller, B.M., Hydrodynamics of steep streams with planar
 1609 coarse-grained beds: Turbulence, flow resistance, and implications for sediment
 1610 transport, *Water Resour. Res.*, 53, 2240-2263, 2017.

1611 Lenzi, M.A., Mao, I., and Comiti, F., When does bedload transport begin in steep
 1612 boulder-bed streams?, *Hydrol. Proc.*, 20, 3517–3533, 2006.

1613 Li, Z., and Komar, P.D., Laboratory measurements of pivoting angles for applications to
 1614 selective entrainment of gravel in a current, *Sedimentology*, 33, 413-423, 1986.

1615 Litty, C., and Schlunegger, F., Controls on pebbles' size and shapes in streams of the
 1616 Swiss Alps, *J. Geol.*, 123, 405-427, 2017.

1617 Matter, A.: *Sedimentologische Untersuchungen im östlichen Napfgebiet (Entlebuch –*
 1618 *Tal der Grossen Fontanne, Kt. Luzern)*, *Eclogae Geol. Helv.*, 57, 315-428, 1964.

1619 McDonald, B.C., and Banerjee, I., Sediments and bedforms on a braided outwash plain,
 1620 *Can. J. Earth Sci.*, 8, 1282-1301, 1971.

1621 Meyer-Peter, E., and Müller, R., Formulas for bedload transport, *Proceedings of the 2nd*
 1622 *meeting of the Int. Assoc. Hydraul. Struct. Res.*, Stockholm, Sweden. Appendix 2,
 1623 39–64, 1948.

1624 Miall, A.D., *Fluvial sedimentology: An historical overview*, in: *Fluvial sedimentology*,
 1625 edited by: Miall, A.D., Mem. Can. Soc. Petrol. Geol., 5, 1-48, 1978.

1626 Middleton, L.T., and Trujillo, A.P., Sedimentology and depositional setting of the upper
 1627 Proterozoic Scanlan Conglomerate, central Arizona. In: *Sedimentology of*
 1628 *gravels and conglomerates*, edited by: Koster, E.H., and Steel, R.J., Mem. Can.
 1629 Soc. Petrol. Geol., 10, 189-202, 1984.

1630 Mueller, E.R., Pitlick, J., and Nelson, J.M., Variation in the reference Shields stress for
 1631 bed load transport in gravel-bed streams and rivers, *Water Resour. Res.*, 41,
 1632 W04006, 2005.

1633 Ockleford, A.-M., and Haynes, H., The impact of stress history on bed structure, *Earth*
 1634 *Surf. Process. Landf.*, 38, 717-727, 2013.

1635 Papaevangelou, G., Evangelides, C., and Tsimopoulos, C., A new explicit relation for
 1636 friction coefficient f in the Darcy-Weisbach equation, *Proc. 10th Conf. Prot.*
 1637 *Restor. Env.*, PRE10, July 6-9, 2010.

- 1638 Paola, C., Heller, P.L., and Angevine, C., The large-scale dynamics of grain-size
1639 variation in alluvial basins, 1: Theory, *Basin Res.*, 4, 73-90, 1992.
- 1640 Paola, C. and Mohring, D., Palaeohydraulics revisited: palaeoslope estimation in
1641 coarse-grained braided rivers. *Basin Res.*, 8, 243-254, 1996.
- 1642 Parker, G., Self-formed straight rivers with equilibrium banks and mobile bed. Part 2.
1643 The gravel river, *J. Fluid Mech.*, 89, 127-146, 1978.
1644 doi:10.1017/S002112078002505.
- 1645 Pettijohn, F.J., *Sedimentary rocks*, Harper and Brothers, New York, 718 pp., 1957.
- 1646 Pfeiffer, A.M., Finnegan, N.J., and Willenbring, J.K., Sediment supply controls
1647 equilibrium channel geometry in gravel rivers, *Proc. Natl. Acad. Sci. U.S.A.*,
1648 114, 3346-3351, 2017.
- 1649 Philips, C.B., and Jerolmack, D.J., Self-organization of river channels as a critical filter
1650 on climate signals, *Science*, 352, 649-697, 2016.
- 1651 Potsma, G., and Roep, T., Resedimented conglomerates in the bottomsets of Gilbert-
1652 type gravel deltas, *J. Sed. Petrol.*, 55, 874-885, 1985.
- 1653 Powell, M.D., Ockleford, A., Rice, S.P., Hillier, J.K., Nguyen, T., Reid, I., Tate, N.J.,
1654 and Ackerley, D., Structural properties of mobile armors formed at different flow
1655 strengths in gravel-bed rivers. *J. Geophys. Res. – Earth Surface*; 121, 1494-
1656 1515, 2016.
- 1657 Rust, B.R., Depositional models for braided alluvium, in: *Fluvial sedimentology*, edited
1658 by: Miall, A.D., *Mem. Can. Soc. Petrol. Geol.*, 5, 221-245, 1978.
- 1659 Rust, B.R., Proximal braidplain deposits in the Middle Devonian Malbaie Formation of
1660 eastern Gaspé, Quebec, Canada, *Sedimentology*, 31, 675-695, 1984.
- 1661 Rust, B.R., and Gostin, V.A., Fossil transverse ribs in Holocene alluvial fan deposits,
1662 Depot Creek, South Australia, *J. Sediment. Petrol.*, 51, 441-444, 1981.
- 1663 Sengupta, S., Studies on orientation and imbrication of pebbles with respect to cross-
1664 stratification, *J. Sed. Petrol.*, 36, 227-237, 1966.
- 1665 Shao, Z., Zhong, J., Li, Y., Mao, C., Liu, S., Ni, L., Tian, Y., Cui, X., Liu, Y., Wang, X.,
1666 Li, W., and Lin, G., Characteristics and sedimentary processes of lamina-
1667 controlled sand-particle imbricate structure in deposits of Lingshan Island,
1668 Qingdao, China, *Sci. China Earth Sci.*, 57, 1061-1076, 2014.
- 1669 Schlunegger, F., Burbank, D.W., Matter, A., Engesser, B., and Mödden, C.,
1670 Magnetostratigraphic calibration of the Oligocene to Middle Miocene (30-15 Ma)
1671 mammal bizones and depositional sequences of the central Swiss Molasse
1672 basin, *Eclogae geol. Helv.*, 89, 753-788, 1996.
- 1673 Schlunegger, F., Jordan, T.E., and Klaper, E.M., Controls of erosional denudation in
1674 the orogeny on foreland basin evolution: The Oligocene central Swiss Molasse
1675 Basin as an example, *Tectonics*, 16, 823-840, 1997.

geo Uni Bern 22.8.2018 10:47

Deleted: Qin, J., Zhong, D., Wang, G., and Ng, S.L., Influence of particle shape on surface roughness: Dissimilar morphological structures formed by man-made and natural gravels, *Geomorphology*, 190, 16-26, 2013. .

- 1682 Schlunegger, F., and Norton, K.P., Climate vs. tectonics: the competing roles of Late
1683 Oligocene warming and Alpine orogenesis in constructing alluvial megafan
1684 sequences in the North Alpine foreland basin, *Basin Res.*, 27, 230-245, 2015.
- 1685 Schlunegger, F., Norton, K.P., Delunel, R., Ehlers, T.A., and Madella, A., Late Miocene
1686 increase in precipitation in the Western Cordillera of the Andes between 18-19°
1687 latitudes inferred from shifts in sedimentation patterns, *Earth Planet. Sci. Lett.*,
1688 462, 157-168, 2017.
- 1689 Schlunegger, F. and Castellort, S., Immediate and delayed signal of slab breakoff in
1690 Oligo/Miocene Molasse deposits from the European Alps, *Sci. Rep.* 6, 31010,
1691 2016.
- 1692 Shaw, J., and Kellerhals, R., Paleohydraulic interpretation of antidune bedforms with
1693 applications to antidunes in gravel, *J. Sediment. Petrol.*, 47, 257-266, 1977.
- 1694 Shields, A., Anwendungen der Aehnlichkeitsmechanik und der Turbulenzforschung
1695 auf die Geschiebebewegung. *Mitt. Preuss. Versuch. Wasserbau Schiffbau*, 26,
1696 Berlin, 1936.
- 1697 Simons, E.V., and Richardson, E.V., Discussion of resistance properties of sediment-
1698 laden streams, *Am. Soc. Civil Eng. Trans.*, 125, 1170-1172, 1960.
- 1699 Sinclair, H.D., and Jaffey, N., Sedimentology of the Indus Group, Ladakh, northern
1700 India: implications for the timing of initiation of the paeo-Indus River. *J. Geol.*
1701 *Soc. London*, 158, 151-162, 2001.
- 1702 Slooman, A., Simpson, G., Castellort, S., and De Boer, P.L., Geological record of
1703 marine tsunami backwash: The role of the hydraulic jump, *Depositional Record*,
1704 1-19, 2018.
- 1705 Spicher, A., Geologische Karte der Schweiz 1:500'000, *Schweiz. Natf. Ges.*, 1980.
- 1706 Spreafico, M., Hodel, H.P., and Kaspar, H., Rauheiten in ausgesuchten
1707 schweizerischen Fließgewässern, *Berichte des BWG, Seri Wasser*, 102 p.,
1708 Bern, 2001.
- 1709 Stürm, B., Die Rigischüttung. *Sedimentpetrographie, Sedimentologie,*
1710 *Paläogeographie, Tektonik*, PhD thesis, Univ. Zürich, Switzerland, 98 p., 1973.
- 1711 Van der Berg, F., and Schlunegger, F., Alluvial cover dynamics in response to floods of
1712 various magnitudes: The effect of the release of glaciogenic material in a Swiss
1713 Alpine catchment, *Geomorphology*, 141, 121-133, 2012.
- 1714 Wickert, A.D., and Schildgen, T.F., Long-profile evolution of transport-limited gravel-bed
1715 rivers, *Earth Surf. Dynam. Discuss.*, doi: org/10.5194/esurf-2018-39.
- 1716 Wong, M., and Parker, G., Reanalysis and correction of bed-load relation of Meyer-
1717 Peter and Müller using their own database, *J. Hydraul. Eng.*, 132, 1159-1168,
1718 2006.
- 1719 Taki, K., and Parker, G., Transportational cyclic steps created by flow over an erodible
1720 bed. Part 1. Experiments, *J. Hydrol. Res.*, 43, 488-501, 2005.

1721 Todd, S.P., Process deduction from fluvial sedimentary structures, in: Advances in
1722 fluvial dynamics and stratigraphy, edited by: Carling, P.A., and Dawson, M.R.,
1723 John Wiley & Sons Ltd, 299-350, 1996.

1724 Trieste, D.J., Evaluation of supercritical/subcritical flows in high-gradient channel, J.
1725 Hydr. Eng., 118, 1107-1118, 1992.

1726 Trieste, D.J., Supercritical flows versus subcritical flows in natural channels, in:
1727 Hydraulic Engineering '94: Proceedings of the 1994 Conference of the
1728 Hydraulics Division, edited by: Cotroneo, G.V., and Rumer, R.R., Am. Soc. Civ.
1729 Eng., New York, 732-736, 1994.

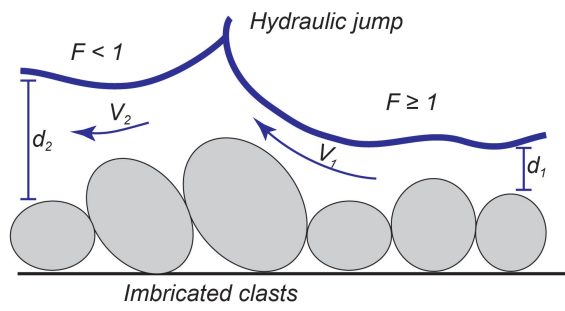
1730 Tucker, G., and Slingerland, R., Drainage basin responses to climate change, Water
1731 Resour. Res., 33, 2031-2047, 1997.

1732 Whipple, K.X., Bedrock rivers and the geomorphology of active orogens, Ann. Rev. Earth
1733 Planet. Sci., 32, 151-185, 2004.

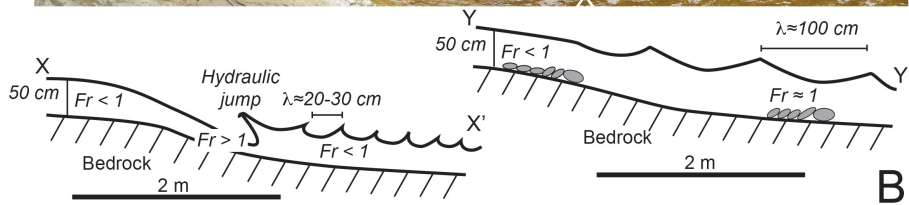
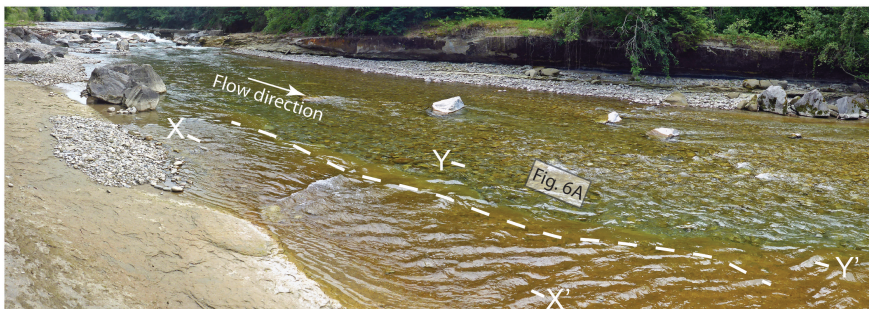
1734 Wiberg, P.L., and Smith, J.D., Velocity distribution and bed roughness in high-gradient
1735 streams, Water Resour. Res., 27, 825-838, 1991.

1736 Yagishita, K., Paleocurrent and fabric analyses of fluvial conglomerates of the
1737 Paeogene Noda Group, northeast Japan, Sed. Geol., 109, 53-71, 1997.

1738



A

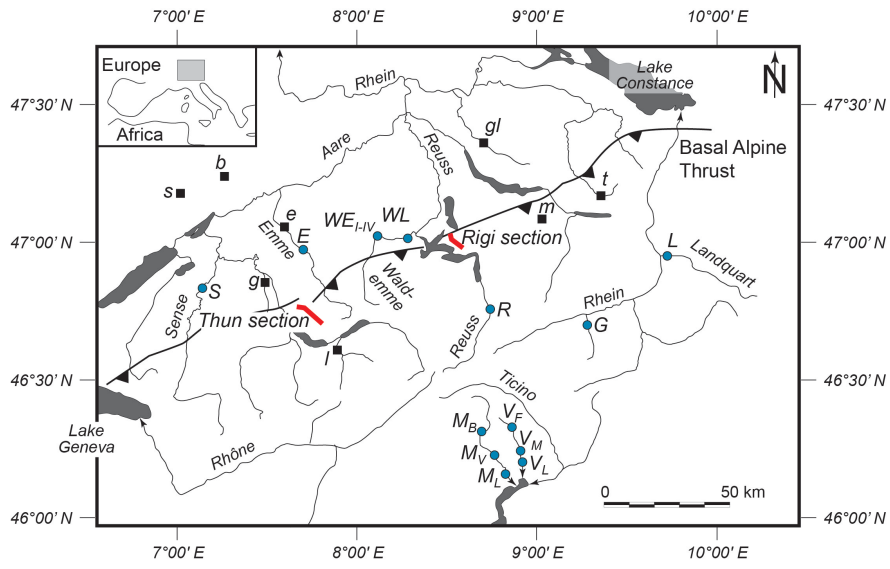


B

1739
1740

Figure 1

Figure 1

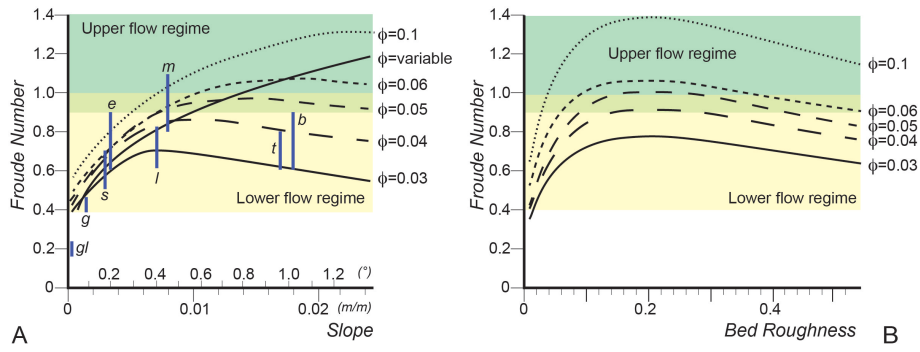


1741

1742 **Figure 2**

1743

Figure 2

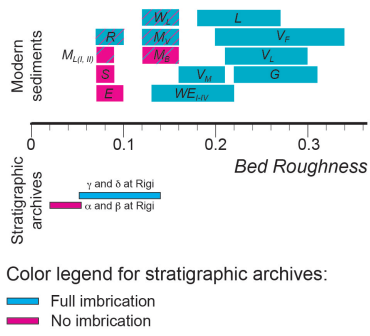
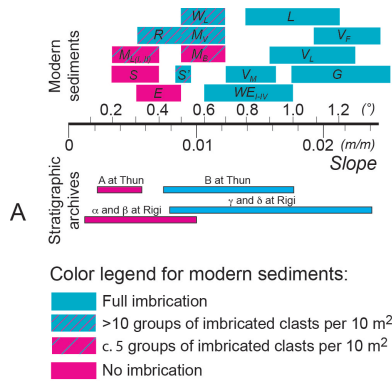


1744

1745 Figure 3

1746

Figure 3



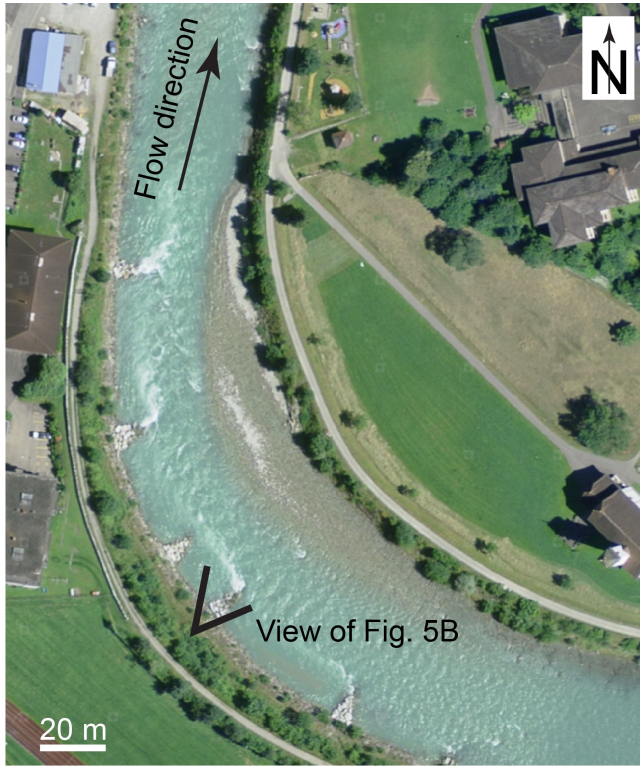
B

Figure 4

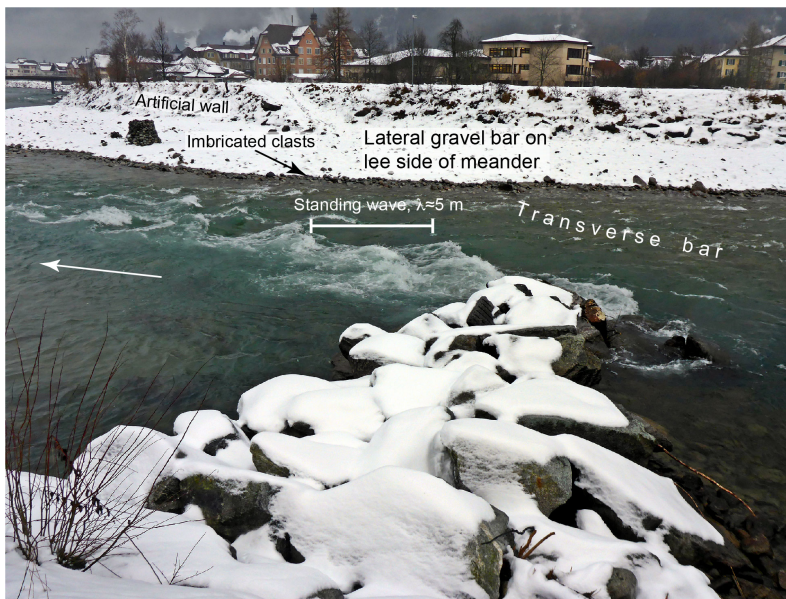
1747

1748 **Figure 4**

1749



A

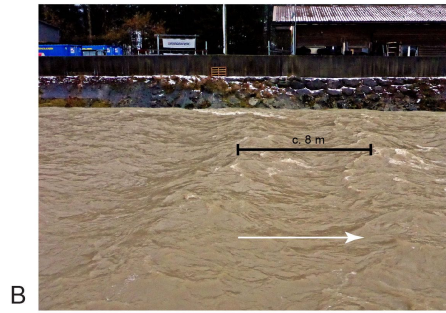
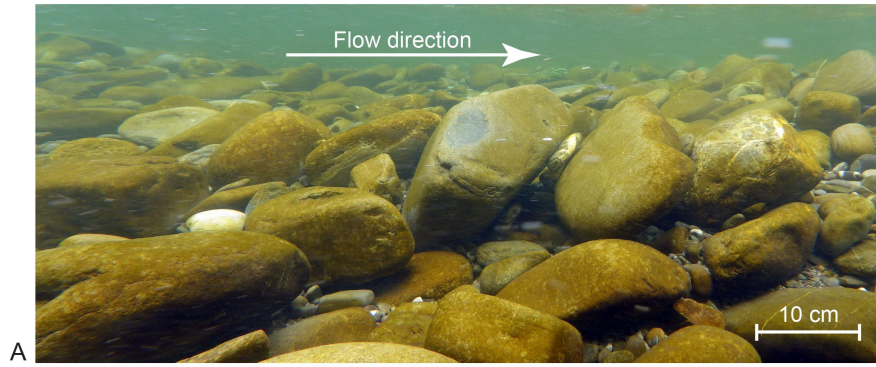


B

1750

1751 Figure 5

1752

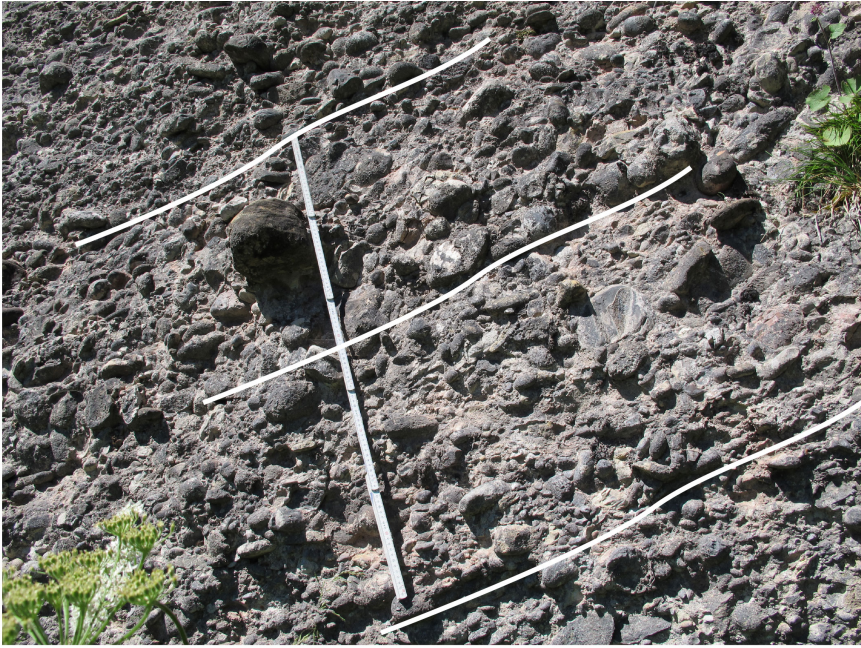


1753

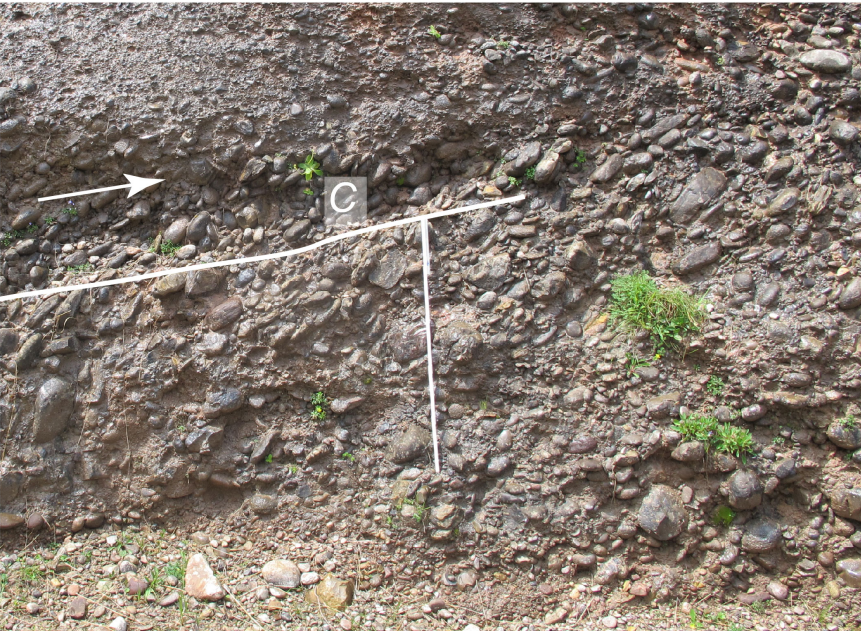
1754 Figure 6

1755

Figure 6



A



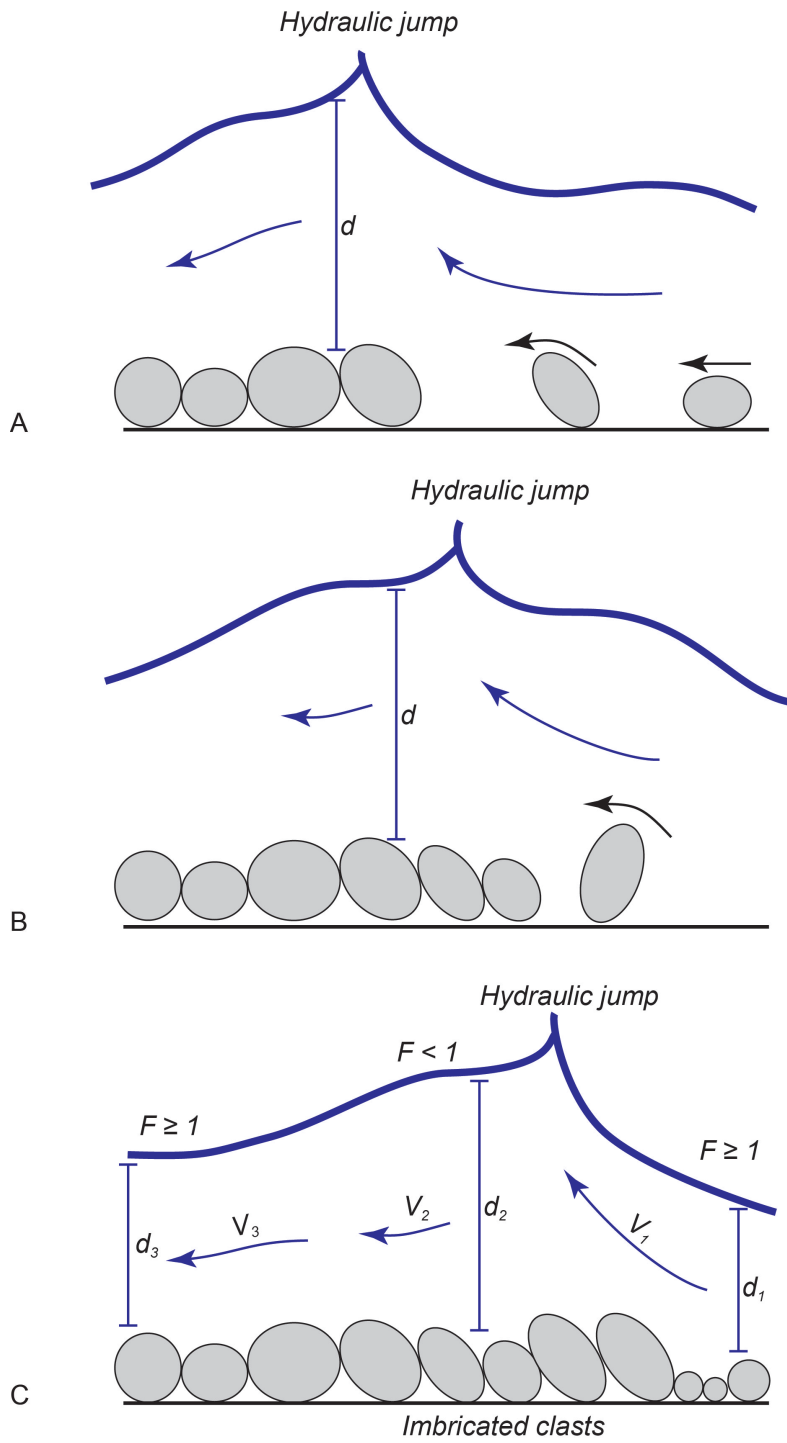
B

1756

1757 Figure 7

1758

Figure 7



1759
1760 Figure 8

Figure 8

Modern gravel bars

Site name	Abbreviation	Site coordinates	D84 (cm)	D50 (cm)	D84/D50	D96 (cm)	Gradient (m/m)	Gradient (°)	Inferred water depth (m)	Roughness	Imbrication
Emme	E	46°57'08N / 7°44'59E	2.3	0.9	2.56	5.2	0.005-0.008	0.4x0.1	0.5-0.8	0.07-0.10	mostly no
Glerner	G	46°44'42N / 8°13'04E	12	3.88	4.17	27.4	0.011-0.024	1.2x0.2	0.4-0.6	0.22-0.31	mostly yes, largest boulders imbricated, smaller pebbles deposited in-between without preferred orientation, sand covers the clay fabric
Landquart	L	46°57'08N / 7°44'59E	10	3.5	4.00	13.5	0.014-0.021	1.0x0.2	0.4-0.6	0.18-0.27	mostly no, but triplets of imbricated clasts occur in places as inferred from photos
Maggia Bignasco	MB	46°44'42N / 8°13'04E	2.7	0.85	3.18	13	0.009-0.012	0.6x0.1	0.2	0.12-0.18	mostly no, but triplets of imbricated clasts occur in places as inferred from photos
Maggia Visio	MV	46°58'28N / 8°36'25E	9.5	2.29	4.15	20	0.009-0.012	0.6x0.1	0.3-0.5	0.12-0.18	mostly yes, triplets and quadruplets of imbricated clasts occur in places
Maggia Losone I	ML I	46°20'08N / 8°36'25E	4	0.79	5.06	14	0.005-0.007	0.3x0.1	0.5-0.6	0.07-0.09	triplets and quadruplets of imbricated clasts occur in places
Maggia Losone II	ML II	46°18'30N / 8°36'25E	6	1.12	5.36	12.85	0.005-0.007	0.3x0.1	0.7-1.0	0.07-0.09	triplets and quadruplets of imbricated clasts occur in places
Verzasca Frasco	VF	46°10'48N / 8°45'33E	2.5	0.75	3.33	7	0.015-0.028	1.3x0.2	0.1	0.03-0.34	imbricated
Verzasca Motta	VM	46°10'15N / 8°49'10E	4.3	1.44	2.99	18.75	0.012-0.016	0.9x0.2	0.2-0.3	0.15-0.21	smaller pebbles deposited in-between without preferred orientation, larger boulders imbricated
Verzasca Lavarlezzo	LV	46°20'20N / 8°48'03E	5	1.3	3.85	30	0.016-0.023	1.1x0.2	0.2-0.3	0.21-0.30	granite boulders above imbricated clasts where no boulders are present
Ruusa	R	46°16'28N / 8°48'34E	3.2	0.88	3.64	6.37	0.005-0.008	0.4x0.1	0.3-0.5	0.07-0.10	imbricated
Sense	S	46°15'21N / 8°50'23E	6	2.42	2.48	9.58	0.005-0.007	0.3x0.1	0.7-1.0	0.07-0.09	in large extent yes triplets and quadruplets of imbricated clasts occur in places. Stream shows standing waves and hydraulic jumps in deep reaches and lower flow regime conditions in flat segments
Waldemne Littau	WL	46°48'53N / 8°39'16E	3.5	0.9	3.89	8.36	0.009-0.012	0.6x0.1	0.2-0.3	0.12-0.18	mostly no, imbrication only at the steep, downstream side faces of transverse bars
Waldemne Entlebuch I	WE I	46°53'20N / 7°20'56E	3	1	3.00	9	0.01-0.017	0.8x0.2	0.1-0.2	0.13-0.22	triplets and quadruplets of imbricated clasts occur in places
Waldemne Entlebuch II	WE II	47°03'04N / 8°15'13E	8	2.43	3.29	18	0.01-0.017	0.8x0.2	0.4-0.6	0.13-0.22	yes
Waldemne Entlebuch III	WE III	47°01'57N / 8°04'03E	5.7	2.07	2.75	14	0.01-0.017	0.8x0.2	0.3-0.5	0.13-0.22	yes
Waldemne Entlebuch IV	WE IV	47°01'57N / 8°04'03E	5.2	2.68	3.08	18	0.01-0.017	0.8x0.2	0.4-0.7	0.13-0.22	yes

Stratigraphic archives

Rigi conglomerates	Segment	D84 (m)	Slope (m/m)	Slope (°)	Inferred water depth (m)	D84/D	Imbrication
a		0.07-0.12	0.009-0.027	0.9x0.4	1.2x0.28	0.05-0.14	yes, in places
b		0.06-0.1	0.008-0.015	0.8x0.2	1.2x0.4	0.04-0.12	partly yes
c		0.04-0.08	0.005-0.011	0.4x0.2	1.7x0.5	0.02-0.05	no
d		0.04-0.08	0.002-0.005	0.2x0.08	2.5x0.8	0.02-0.04	no

Thun conglomerates	Unit	D84 (m)	Slope (m/m)	Slope (°)	Inferred water depth (m)	D84/D	Imbrication
G		not available	0.008-0.017	0.7x0.3	1.5-2	not available	yes, in places
A		not available	0.003-0.005	0.2x0.1	3-5	not available	no

Modern gravel bars

Site name	Abbreviation	Site coordinates	D84 (cm)	D50 (cm)	D84/D50	D96 (cm)	Gradient (m/m)	Gradient (°)	Inferred water depth (m)	Roughness	Imbrication
Emme	E	46°57'08N / 7°44'59E	2.3	0.9	2.56	5.2	0.005-0.008	0.4x0.1	0.5-0.8	0.07-0.10	mostly no
Glerner	G	46°44'42N / 8°13'04E	12	3.88	4.17	27.4	0.011-0.024	1.2x0.2	0.4-0.6	0.22-0.31	mostly yes, largest boulders imbricated, smaller pebbles deposited in-between without preferred orientation, sand covers the clay fabric
Landquart	L	46°57'08N / 7°44'59E	10	3.5	4.00	13.5	0.014-0.021	1.0x0.2	0.4-0.6	0.18-0.27	mostly no, but triplets of imbricated clasts occur in places as inferred from photos
Maggia Bignasco	MB	46°44'42N / 8°13'04E	2.7	0.85	3.18	13	0.009-0.012	0.6x0.1	0.2	0.12-0.18	mostly no, but triplets of imbricated clasts occur in places as inferred from photos
Maggia Visio	MV	46°58'28N / 8°36'25E	9.5	2.29	4.15	20	0.009-0.012	0.6x0.1	0.3-0.5	0.12-0.18	mostly yes, triplets and quadruplets of imbricated clasts occur in places
Maggia Losone I	ML I	46°20'08N / 8°36'25E	4	0.79	5.06	14	0.005-0.007	0.3x0.1	0.5-0.6	0.07-0.09	triplets and quadruplets of imbricated clasts occur in places
Maggia Losone II	ML II	46°18'30N / 8°36'25E	6	1.12	5.36	12.85	0.005-0.007	0.3x0.1	0.7-1.0	0.07-0.09	triplets and quadruplets of imbricated clasts occur in places
Verzasca Frasco	VF	46°10'48N / 8°45'33E	2.5	0.75	3.33	7	0.015-0.028	1.3x0.2	0.1	0.03-0.34	imbricated
Verzasca Motta	VM	46°10'15N / 8°49'10E	4.3	1.44	2.99	18.75	0.012-0.016	0.9x0.2	0.2-0.3	0.15-0.21	smaller pebbles deposited in-between without preferred orientation, larger boulders imbricated
Verzasca Lavarlezzo	LV	46°20'20N / 8°48'03E	5	1.3	3.85	30	0.016-0.023	1.1x0.2	0.2-0.3	0.21-0.30	granite boulders above imbricated clasts where no boulders are present
Ruusa	R	46°16'28N / 8°48'34E	3.2	0.88	3.64	6.37	0.005-0.008	0.4x0.1	0.3-0.5	0.07-0.10	imbricated
Sense	S	46°15'21N / 8°50'23E	6	2.42	2.48	9.58	0.005-0.007	0.3x0.1	0.7-1.0	0.07-0.09	in large extent yes triplets and quadruplets of imbricated clasts occur in places. Stream shows standing waves and hydraulic jumps in deep reaches and lower flow regime conditions in flat segments
Waldemne Littau	WL	46°48'53N / 8°39'16E	3.5	0.9	3.89	8.36	0.009-0.012	0.6x0.1	0.2-0.3	0.12-0.18	mostly no, imbrication only at the steep, downstream side faces of transverse bars
Waldemne Entlebuch I	WE I	46°53'20N / 7°20'56E	3	1	3.00	9	0.01-0.017	0.8x0.2	0.1-0.2	0.13-0.22	triplets and quadruplets of imbricated clasts occur in places
Waldemne Entlebuch II	WE II	47°03'04N / 8°15'13E	8	2.43	3.29	18	0.01-0.017	0.8x0.2	0.4-0.6	0.13-0.22	yes
Waldemne Entlebuch III	WE III	47°01'57N / 8°04'03E	5.7	2.07	2.75	14	0.01-0.017	0.8x0.2	0.3-0.5	0.13-0.22	yes
Waldemne Entlebuch IV	WE IV	47°01'57N / 8°04'03E	5.2	2.68	3.08	18	0.01-0.017	0.8x0.2	0.4-0.7	0.13-0.22	yes

Stratigraphic archives

Rigi conglomerates	Segment	D84 (m)	Slope (m/m)	Sk
a		0.07-0.12	0.009-0.027	0.6
b		0.06-0.1	0.008-0.015	0.6
c		0.04-0.08	0.005-0.011	0.4
d		0.04-0.08	0.002-0.005	0.2

Thun conglomerates	Unit	D84 (m)	Slope (m/m)	Sk
G		not available	0.008-0.017	0.1
A		not available	0.003-0.005	0.2

Deleted:

1761
1762
1763

Table 1